EE

Technical Report
RAL-TR-1998-019

SW9821

Muon Facilities and Experiments; Now and in the New Millennium

G H Eaton

April 1998

COUNCIL FOR THE CENTRAL LABORATORY OF THE RESEARCH COUNCILS

Enquiries about copyright, reproduction and requests for additional copies of this report should be addressed to:

The Central Laboratory of the Research Councils
Library and Information Services
Rutherford Appleton Laboratory
Chilton
Didcot
Oxfordshire
OX11 0QX
Tel: 01235 445384 Fax: 01235 446403
E-mail library@rl.ac.uk

ISSN 1358-6254

RAL Report
RAL-TR-98-019

Muon Facilities and Experiments; Now and in the New Millennium

G. H. Eaton

Lectures given at the Nato Advanced Study Institute on Muon Science

SUSSP 51 Scottish Universities Summer School in Physics

University of St Andrews

Scotland, U.K.

17 - 28 August 1998

April 1998

Rutherford Appleton Laboratory, Chilton, Didcot, Oxfordshire OX11 0QX.

Index **Page**

The Muon: A case of the Cavemans Fire

As all of you are aware, enormous progress has been made over the last century or so in our scientific understanding of the universe of which we find ourselves. But on a personal note it seems to me that while our accumulated factual knowledge has indeed expanded to a level undreamed of just a few generations back both on the scale of the universe itself and on the microscopic scale involved in elementary particle physics, our basic understanding of many of these phenomena is still elementary and many questions still await an answer.

A good and highly relevant (to attendees of this summer school) example of this incomplete understanding is the muon itself. We now routinely use this elementary particle in our scientific studies as a tool for materials science, molecular science and in fundamental studies of basic processes involving sub nuclear particles.

This is like one of our caveman ancestors many thousand of years ago, who is contentedly cooking his woolly mammoth steak on the recently discovered fire. Like the muon he recognises the usefulness of his fire, but has no understanding of what the fire is and what is going on in its glowing embers. Nevertheless undeterred he continues to use it and is not too bothered intellectually by his inability to explain to his offspring the nature of the new discovery.

We are in a similar position with regard to our use of muons as a scientific tool. While the properties of this particle have been well established, why many of these are what they are remain a mystery as I will point out during these lectures. Nevertheless let us not be deterred from using these new particles as a tool to understanding and unravelling many scientific problems, in the best traditions of our forefathers, however we should retain the humility of our present day ignorance of the important and intricate secrets responsible for the properties of the lepton family of elementary particles of which the muon is a member.

First steps in Muon Science: The Discovery of the pion and muon.

The muon was first seen in a Wilson cloud chamber exposed to cosmic rays by Kunze [1] in 1933 in a photograph shown in figure (1). One can see in this figure, an electron and a considerably stronger ionising particle of smaller curvature. He said at the time that the nature of this particle is unknown, since it ionises too little for a proton and too much for an electron. Attributing this particle to something originating in a nuclear explosion, he failed to claim the discovery of a new elementary particle.

The definitive discovery of the muon occurred three years later when Neddermeyer and Anderson [2] again using a Wilson cloud chamber carried out measurements of the energy loss of particles occurring in cosmic ray showers in heavy materials like platinum. They observed particles which penetrated the absorber more strongly than electrons leading to the

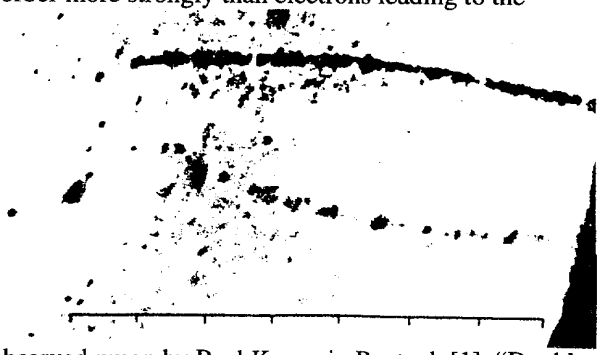

Fig. 1. The first observed muon by Paul Kunze in Rostock [1]: "Double track as a result of a probable nuclear explosion. Lower track: electron of 37 000 000 V. The nature of the upper positive particle is unknown."

conclusion that they were particles of unit charge with a mass larger than electrons but much smaller than protons.

The initial hope was that the new particle was that responsible for the strong nuclear force as predicted in Yukawa in 1935 [3]. It was even observed that the new particle decayed into an electron, as postulated by Yukawa to explain beta-decay. However it soon became apparent from the work of Conversi, Pancini and Piccioni [4] that the new mesotron appeared to have a very weak nuclear interaction with matter in contradiction to the essential predicted property of the Yukawa particle.

Theoretical suggestions by Tanikawa and Sakata and Inoue [5] that the explanation of these mysteries lay in a two meson hypothesis with a Yukawa type strongly interacting meson (pion) decaying to a weakly interacting mesotron were finally verified experimentally by Powell and his collaborators in Bristol [6]. Using nuclear emulsions they observed a number of two meson decay events, one of which is shown in figure (2).

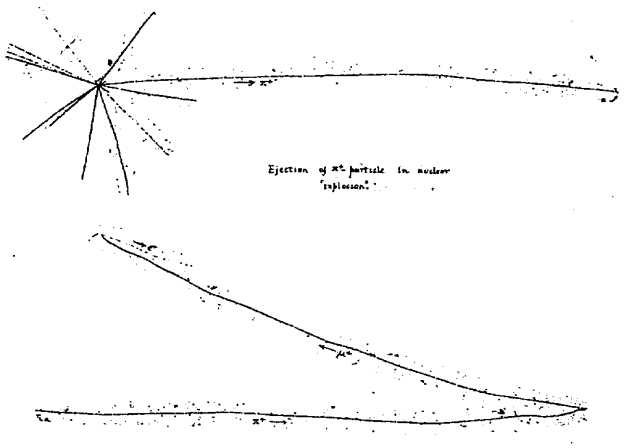

Fig (2) Emulsion exposure showing a two meson event. The track of the positively charged pion is emitted from a cosmic ray induced nuclear interaction, and bottom right the pion decays into a muon which after 600 microns travel, decays itself into a positron.

All of the events seen, displayed a constant range for the secondary muon of about 600 microns in the emulsion, leading to the conclusion of a two-body decay of the primary meson, called the π or pion, to a secondary meson, μ or muon and one neutral particle. Twenty such events enabled mass estimates of 260 ± 30 and 205 ± 30 electron masses for the pion and muon, and approximately 10^{-8} seconds for the pion lifetime.

This research verified that muons were born from the decay of the pion, the particle responsible for the strong force in nuclei, but that the muon was quite unique in its properties; no strong interaction, two kinds with opposite charges $\mu\pm$, a long lifetime of μsecs and properties similar to that of the electron but two hundred times as heavy. It is understandable that many physicists of the time from Rabi to Gell-Mann and Rosenbaum did not place a welcome mat for the new particle, signifying as it did, the end of innocence in their current understanding of particle physics [7, 8]. As I remarked at the beginning, some of these properties of the muon are still not understood.

All of the experiments hitherto described were carried out with cosmic ray produced muons. Major advances in muon science and their application followed from the first production of pions and muons by particle accelerators about 1957. All of our current research use accelerator based muon facilities, now second generation facilities following on from the early accelerators.

a) Pion Production

In the Yukawa model, the nuclear force binding nuclei together can be described by the exchange of a quantum from one nucleon, which is immediately absorbed by another, analogous to the force between electrically charged particles as being due to the exchange of a massless photon. Because the nuclear force was shown to be short ranged (~ 10^{-13} cm), the mass of this exchanged quantum or pion has to be ~ 200 electron masses.

An isolated stationary nucleon cannot emit or absorb a pion and conserve energy and momentum in the process. However energy conservation can be violated by an amount ΔE for a time Δt if $\Delta E.\ \Delta t \sim \hbar$, given by the Heisenberg Uncertainty principle. With a pion mass of ~ 140 MeV equivalent to ΔE, then Δt has to be of the order of 4 10^{-24} secs, during which time the pion can travel a distance of $\hbar$/mc. In this way one can picture a nucleon being surrounded by a virtual cloud of pions, giving a characteristic charge distribution of RMS radius 0.8f and magnetic moment of + 2.79 nuclear magnetons.

In order to produce pions external to the nucleon itself one has to bombard necleons with other nucleons of sufficient kinetic energy such that the available centre of mass energy is greater than the pion mass of 140 MeV. Typical nucleon-nucleon reactions producing pions are the following,

$$\begin{aligned} p + p &\rightarrow p + n + \pi^+ \qquad p + p \rightarrow d + \pi^+ \\ &\rightarrow p + p + \pi^0 \\ p + n &\rightarrow p + n + \pi^0 \\ &\rightarrow p + p + \pi^- \\ &\quad n + n + \pi^+ \end{aligned}$$

These reactions are termed single pion production and have an energy threshold of approximately 280 MeV in the laboratory. However the probability (or cross sections) for producing pions in such reactions increases rapidly if more energy is available as shown in Figure (3). [9, 10] This shows that to get the maximum number of single pions using proton beams from an accelerator then one should aim for a 500 MeV to 1000 MeV energy range. (the so called intermediate energy range.) This defines the optimal energy for an accelerator based pion (and muon) source.

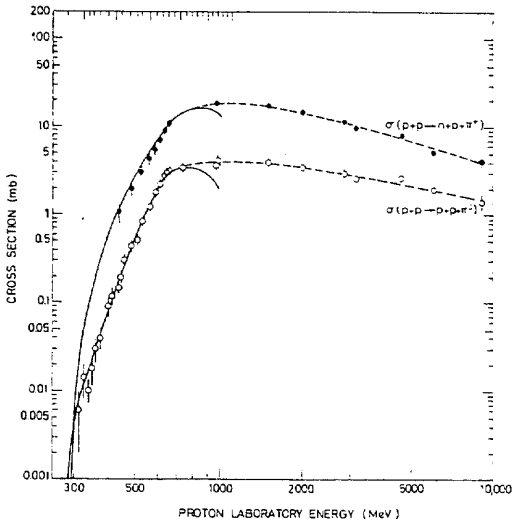

Fig 3: Cross-sections for single pion production.

The reactions above, which result in a final configuration of three particles (eg pπn etc) produce a broad distribution of pion energies, typically peaked at ~ 200 MeV for incident protons of 600 MeV. The two body production process,

$$p + p \rightarrow d + \pi^+$$

gives a monoenergetic pion beam of 300 MeV at forward angles for the same proton energy. The cross section for this reaction as a function of proton energy is shown in figure (4).

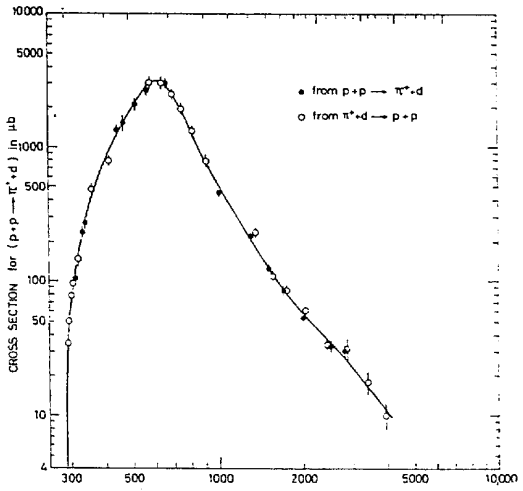

Fig 4. Cross-section for the reaction ($p+p \rightarrow \pi^+ + d$) including data obtained from the reverse reaction, assuming detailed balance.

Typical energy spectra of pions produced by various energy protons incident on carbon are shown in figure (5).

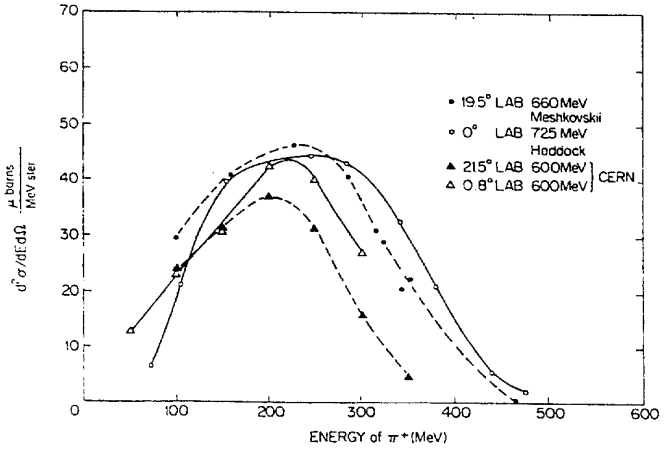

Fig. 5. Energy Spectra of π^+ produced in proton-carbon collisions.

In addition to producing pions singly, it is possible given as accelerator of sufficient energy, to produce pions in pairs as the reactions below,

In addition to producing pions singly, it is possible given as accelerator of sufficient energy, to produce pions in pairs as the reactions below,

$$
\begin{aligned}
p + p &\rightarrow p + p + \pi^+ + \pi^- \\
&\quad p + p + \pi^\circ + \pi^\circ \\
&\quad n + \pi + \pi^+ + \pi^+ \\
&\quad n + p + \pi^+ + \pi^\circ \\
&\quad d + \pi^+ + \pi^\circ
\end{aligned}
\qquad
\begin{aligned}
p + n &\rightarrow p + n + \pi^+ + \pi^- \\
&\quad p + n + \pi^\circ + \pi^\circ \\
&\quad n + n + \pi^+ + \pi^\circ \\
&\quad p + p + \pi^- + \pi^\circ \\
&\quad d + \pi^+ + \pi^- \\
&\quad d + \pi^\circ + \pi^\circ
\end{aligned}
$$

Not surprisingly, more powerful accelerators are needed to do this as can be seen from Figure (6), which shows the double pion production cross sections again as a function of laboratory kinetic energy of the bombarding protons [11]. These reactions have a threshold kinetic energy in the lab of 600MeV, with cross sections reaching saturation levels above 1.5 - 2.0 GeV. Future accelerator based muon sources will probably be in this energy regime and benefit from double pion contributions to the pion and hence muon production rates.

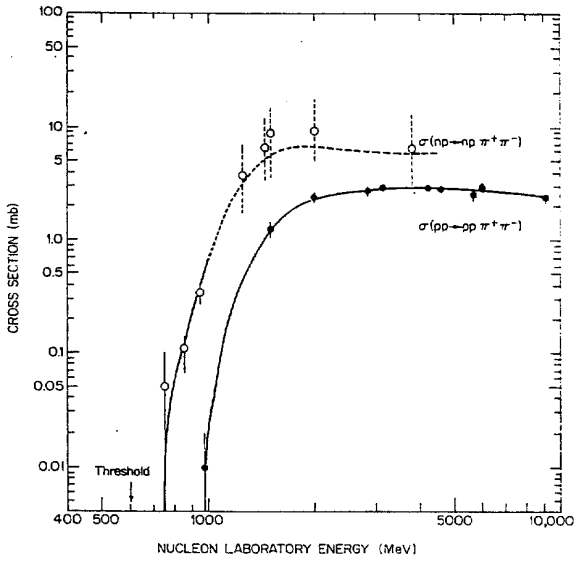

Fig. 6. Examples of cross-sections for double pion production.

b) Accelerators for Muon Facilities

After 1957, the first generation of proton accelerators capable of providing intense beams of pions and hence muons, became available. With these accelerators great advances in muon research were achieved and the embryonic sciences of muon spin rotation (μSR), muon catalysed nuclear fusion (μCF) and fundamental particle physics with muons were born. These early accelerators notably the Nevis Columbia, SREL Berkeley USA and CERN Synchrocyclotrons, were followed in 1974 by the second generation meson factories at Los Alamos, SIN (PSI) Zurich Switzerland and TRIUMF Vancouver, which were more than two order of magnitude more intense and established muon science on the fine footing it enjoys today. These continuous (or quasi continuous) sources were followed in 1981 by the pulsed

facility (BOOM) in Japan, and finally in 1987 by the worlds most intense pulsed facility at ISIS in the UK. Table 1 shows a compilation of first and second generation accelerators.

At the present time, most of the research with muons is conducted at the muon facilities at PSI and TRIUMF, both continuous sources, and at the pulsed muon facility at ISIS. It can be expected that these facilities will continue to operate for a period of 10 - 15 years from now, so many of the students here might well find themselves using these facilities, which I will describe in some detail. The next generation of sources i.e the ESS (European Spallation Source) and the JHF (Japanese Hadron Facility) will come on line in ~2005.

It is interesting here to point out that ISIS and ESS are designed as spallation neutron sources, where intense pulsed proton beams are used to produce intense pulses of neutrons from the spallation reaction in heavy metal targets. Why then are they suitable as sources for pions and muons particularly with regard to the energy of the machine.

Table 1 . Table of intermediate energy accelerators yielding proton energies > 100 MeV

Accelerator and location	*Present energy (MeV)*	*Date of first operation*
Sector-focused cyclotrons		
Univ. of Maryland, USA	140 (p)	1968
Triumf, Vancouver, Canada	500 (H^-)	1973(?)
Sector-focused ring cyclotrons		
Univ. of Indiana, USA	200 (p)	1972(?)
Zürich, Switzerland	520	1974(?)
Proton synchrocyclotrons		
McGill Univ., Canada	100	1949
Harvard Univ., USA	160	1949
Harwell, UK	160	1949
Orsay, France	160	1958
Uppsala, Sweden	185	1951
Rochester, USA	240	1948†
Liverpool, UK	380	1954†
Columbia Univ., USA	385	1950
Carnegie-Mellon Univ., USA	440	1951
Chicago, USA	460	1951
CERN, Switzerland	600	1957
SREL, Newport News, USA	600	1966
Dubna, USSR	680 (p)	1949
Berkeley, USA	740 (p)	1946
Gatchina, USSR	1000	1968
Proton linear accelerator		
Los Alamos, USA	800	1972(?)
Proton synchrotrons		
Birmingham, UK	1,000	1953†
Brookhaven, USA	3,000	1952†
Saclay, France	3,000	1958
Princeton, USA	3,000	1963
Berkeley, USA	6,200	1954
Chilton, UK	7,000	1963
Moscow, USSR	7,000	1961
Dubna, USSR	10,000	1957
Argonne, USA	12,500	1963
CERN, Switzerland	28,000	1959
Brookhaven, USA	33,000	1960
Serpukhov, USSR	76,000	1967
Batavia, USA	200,000	1972(?)

The meson factories at TRIUMF (500 MeV) and Los Alamos (800 MeV) were designed with an energy suitable to provide the maximum pion and muon fluxes as indicated in figures 3 and 4. Fortunately for us muon scientists, it turns out that the required energy of accelerator based spallation neutron sources is similar to the optimum required for meson factories. This can be seen from figure (7), which shows the energy dependence of the number of spallation neutrons produced per proton from various heavy targets. This increases linearly with energy from 300 MeV to 1000 MeV, so that ISIS is based upon a selected energy of 800 MeV protons, ideal for an intense muon source. ESS has chosen 1.33 GeV which affords intensity

gains based on multi-pion production discussed previously. Since it is expected that future intermediate energy high intensity accelerators will be predominantly built as spallation neutron sources, it looks as if muon science will continue to flourish at such facilities.

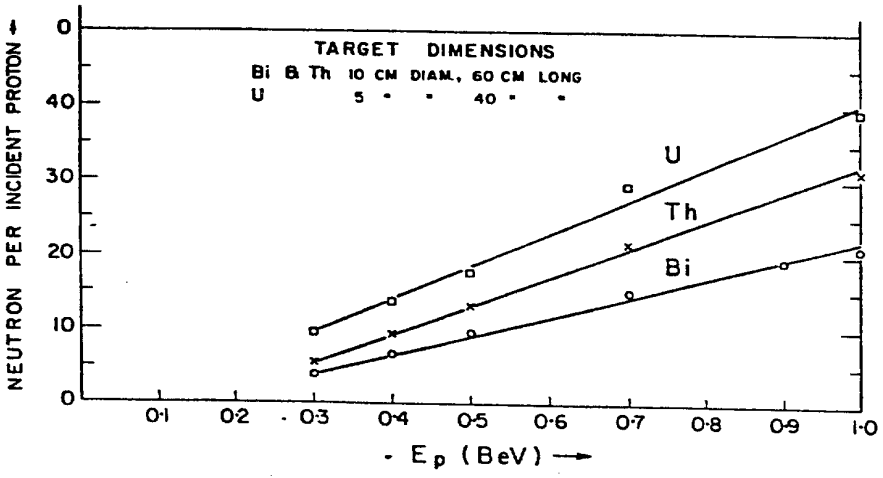

Fig. 7: Total number of neutrons produced (including the high energy cascades) by protons incident along the axis of the targets as a function of the incident proton energy.

Properties of the Pion and Pion Decay

The properties of the pions produced in the reactions discussed hitherto are summarized below.

Charge States	π^+	π^-	π^o
Mean life (secs)	26.04×10^{-9}	26.04×10^{-9}	0.89×10^{-16}
Spin	0	0	0
Mass (MeV) [12]	139.5679	139.5679	134.97
Decay modes	$\pi^+ \rightarrow \mu^+ + \nu_\mu$	$\pi^- \rightarrow \mu^- + \bar{\nu}_\mu$	$\pi^o \rightarrow \gamma + \gamma$
	(weak decay)		

The pion mass of 139.577 MeV can be compared with 0.511 MeV for the electron and 938.26 MeV for the proton. The mean life of the charged pion is 26 ns, an important factor to be considered later in this paper. The positive pion decays via the weak interaction with this lifetime into a positive μ (muon) and a massless (?) muon neutrino [negative pions decay into μ^- and a muon anti neutrino]. Other pion decay modes are negligible at the 10^{-4} level.

The two decay process of a charged pion (mass 139.5679 MeV) into a muon (mass 105.65946 MeV) [12] and a supposed massless neutrino, results in a unique energy and momentum (4.1 MeV and 29.7877 MeV/c) for the muon emerging from the reaction if the parent pion is at rest. A precise measurement [13] of the muon momentum from this decay process provides to date the best upper limit yet available for the muon neutrino mass [13].

The spin of the pion is zero as deduced from the lack of fine structure in π mesic x-rays [14].

The neutrino is an uncharged particle originally postulated by Pauli to describe the energy spectrum of electrons observed in radioactive βeta decay. At the present time these neutrinos have been observed in various accelerator labs although for many years this observation was not possible.

It is now known that neutrinos come in two types, one associated with electrons (ν_e) and the other with muons (ν_μ), each one having its own anti-particle ($\overline{\nu}_e$) ($\overline{\nu}_\mu$) which are different from its corresponding neutrino.

As yet no neutrino mass has been detected, although much effort has been extended in these experiments.

The spin of both neutrinos is ½. For neutrinos the spin and momentum are antiparallel (ie the neutrino has a left handed spin), while for antineutrinos the spin and momentum are parallel (ie the antineutrino has a right handed spin). These properties are usually described as helicity, with antineutrinos having as helicity of + 1, while neutrinos have an helicity of - 1. The fact that neutrinos emitted is π^+ decay can only have a negative helicity is a direct result of parity violation in the weak interaction . In the decay process at rest $\pi^+ \rightarrow \mu^+ + \nu_\mu$, the muon and neutrino have opposite momentum (to conserve momentum), so that it follows that the muon and neutrino must have anti parallel spins to conserve angular momentum in the decay. This is shown in figure (8).

Fig.8. : Decay of the positive pion in a coordinate system where the pion is at rest.
Directions of spin and momentum for the decay particles are indicated.

The muons produced in pion decay at rest are emitted isotropically in space. As outlined above because the decay process is via the weak interaction (and hence parity violating), the neutrino spin s_ν is in the opposite direction to its momentum p_ν. Since the pion has zero spin, the muon is forced to have its spin opposite to its propagation direction. Hence the muons emitted in any direction of choice must be 100% polarized (all spinning in the same direction), a vital ingredient for their use in muon spin rotation.

Properties of the Muon and Muon Decay

The properties of the muon and muon decay are shown in Table

Property	Value
Mass	105·6595 (3) MeV =206·7684 (6) M_e =0·1126 M_p
Charge	±e
Spin	½
Magnetic moment	μ_μ=3·1833448 (29) μ_p
Gyromagnetic ratio	γ_μ=13·55×10³ Hz/G
Average lifetime	τ_μ=2·1994 (6) μs
Decay modes	$\mu^+ \rightarrow e^+ + \nu_e + \bar{\nu}_\mu$ $\mu^- \rightarrow e^- + \bar{\nu}_e + \nu_\mu$
Angular distribution	$dN_{e\pm} \approx$ $(1 \pm A \cos\theta)\, d\Omega$ $A \approx 0{\cdot}3, \theta = \sphericalangle (\boldsymbol{S}_\mu, \boldsymbol{P}_{e\pm})$
Production	$\pi^\pm \rightarrow \mu^\pm + \nu_\mu(\bar{\nu}_\mu)$ $\tau_\pi = 2{\cdot}2 \times 10^{-8}$ s

The decay of the muon into an electron and neutral particle(s) is again via the weak interaction process and occurs with a muon life time of 2.2 10^{-6} seconds (2.2 μsecs). In contrast of pion decay which produces a monoenergetic muon which implies a two body decay process, the decay of a muon produces a broad energy spectrum of the emitted electron [15], hence implying that two neutral particles must be associated with the muon. The measured momentum spectrum of the electron (Michel Spectrum) is shown in figure (9), showing a broad distribution extending to a maximum value of p_e = 52.9 MeV/c.

This evidence led to the establishment of the following decay process.

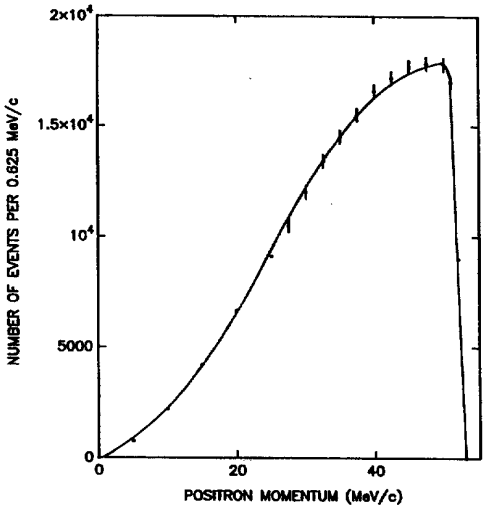

Fig.9. :Momentum spectrum of positrons from muon decay.

$$\mu^+ \rightarrow e^+ + \nu_e + \bar{\nu}_\mu \qquad \mu^- \rightarrow e^- + \bar{\nu}_e + \nu_\mu$$

The peaking of the energy spectrum at the high energy end implies that the two neutrinos are emitted preferentially in the opposite direction of the electron as shown in figure (10) where the decay energy is shared between the positron and the two neutrinos. The fact that in this decay process, two different types of neutrinos are involved, ie ν_e and ν_μ followed from the non-observation of the $\mu^+ \rightarrow e + \gamma$ process, which would be possible if annihilation occurred of identical neutrino types in muon decay.

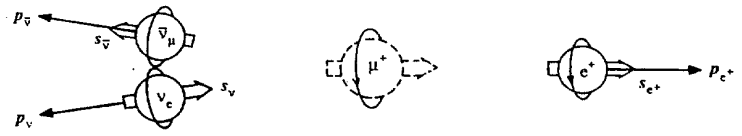

Fig 10. conservation of angular and linear momentum when the positron energy is close to the maximum value E_{max} and the two neutrinos are emitted in approximately the same direction.

Angular distribution of Electrons in Muon Decay: The basis for Muon-spin-rotation.

Because of parity violation in muon decay via the weak interaction the angular distribution $W(\theta)$ of the positron is strongly anisotropic with respect to the muon spin. This asymmetry has a maximum at $\varepsilon_e = \varepsilon_{max}$ because the electron is emitted in exactly the opposite direction to the two neutrinos (figure (10)). This conclusion follows from the fact that since the positron has positive helicity and the spins of the two neutrinos add to zero, the positron must be emitted predominantly in the direction of the muon spin.

Indeed by observing this asymmetry, parity violation in the weak decay of the π and μ was first established [16].

If instead of detecting only positrons near the end of the Michel spectrum, we observe them with all energies, then the overall asymmetry with respect to the muon spin is reduced with an angular distribution of the form:

$$W(\theta) = 1 + a_o \cos\theta$$

where $W(\theta)$ is the angular distribution of the emitted positron with respect to the muon spin, and a_o is the asymmetry parameter. The theoretical value of a_o is 1/3. Figure (11) shows the angular distributions for a) only maximum energy positrons are detected and b) all energies of positrons are detected.

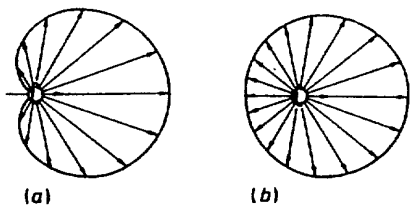

Fig 11. : Angular distributions expected for the emitted positrons (with reference to the muon spin direction) when (a) only positrons with energy E_{max} are detected and (b) positrons of all energies are included.

The critical fact that parity violation in weak interactions responsible for both pion π and muon decay produces in the first case, polarised muons and secondly that the electron from the subsequent muon decay tends to reflect the muon spin direction form the major requirement for the use of muons in μSR studies in materials science. Also highly relevant to μSR studies is the magnetic moment (8.90 μ_N) and mass (0.11 M_p).

The muon lifetime itself is very long (2.2 μsecs) compared with those for other unstable elementary particles and opens up a unique time window for μSR studies.

These significant facts are important for μSR can be extended to the muon mass itself, which is just that required for fast resonant formation of deuterium-tritium molecules bound by a muon (10^{-9}secs), (a critical factor in muon catalysed fusion studies). The long muon lifetime in principle would allow one single muon to catalyse a thousand or more dt fusions, leading to a solution of the worlds energy problems [17].

Muon Facilities for Muon Science

Introduction

The requirement for μSR science is to make available, intense beams of polarized muons of both charge signs, although as we will see from other lectures, the predominant usage is for positively charged muons. Muon catalyzed fusion research requires negative muons where the polarization is immaterial. Fundamental physics experiments with muons have similar requirements to those for μSR.

At the present time, the principal continuous muon sources are at TRIUMF [18] and PSI [19], while the pulsed facilities are at KEK [20] and ISIS [21]. In these lectures I will concentrate on describing in detail the muon facilities at ISIS, and during each topic I will point out any significant differences between this pulsed source and the continuous sources at the meson factories PSI and TRIUMF. I will start at the point where all muon facilities begin, namely the production target in the proton beam from which all muon facilities derive the pions which are therein produced and hence the muons themselves . But even before we consider the production target, we must first refer to the characteristics of the proton beam produced from the accelerator in question, particularly the time structure of this beam, as this directly effects the time structure of the muon facility and its associated experiments.

The ISIS Proton Synchrotron and Extracted Proton beam.

The ISIS Spallation Neutron source is shown in figure (12).

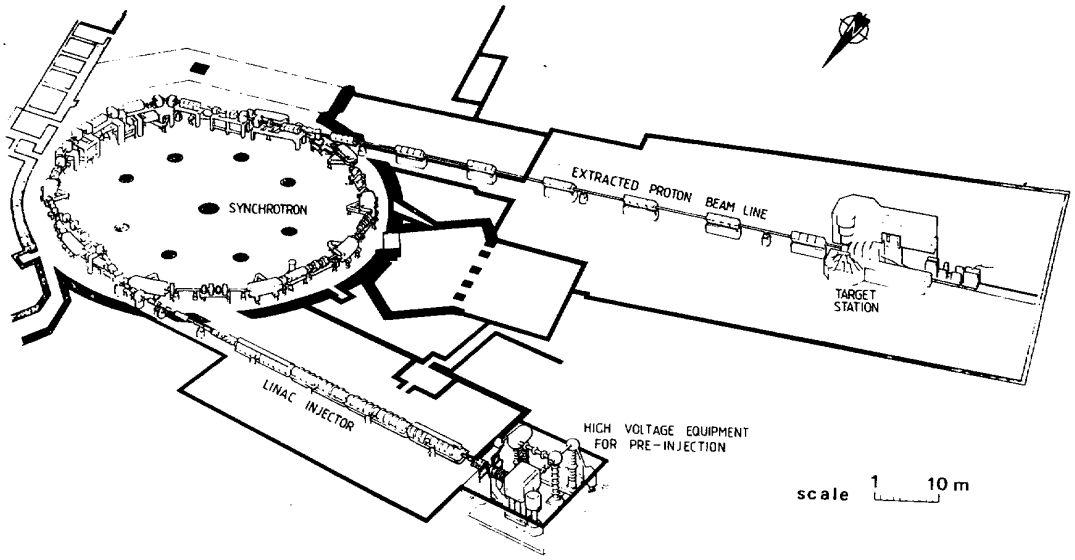

Fig : 12. Lay-out of the Rutherford Appleton Laboratory Spallation Neutron Source, showing the Linac injector, synchnotron, extracted proton beam and spallation neutron target station. The muon beams are generated from an intermediate target 20 m upstream of the main ISIS target.

The principal component of this facility consists of a rapid cycling proton synchnotron which produces a high intensity 200μA (1.2 10^{15} pps) proton beam at 800 MeV, which is used in conjunction with a heavy stopping target to create intense beams of pulsed neutrons by the spallation process. The ISIS synchnotron produces pulses of protons at 50 Hz, but because the machine operates at twice the circulation frequency of the protons, it eventually produces a double pulsed proton beam with a time structure shown in figure (13).

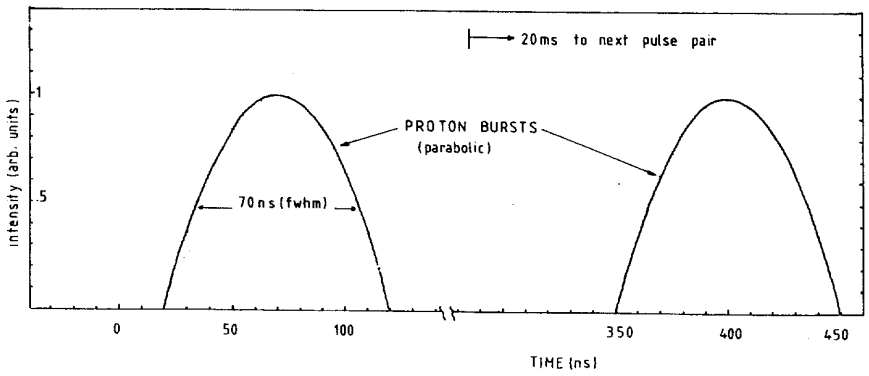

Fig. 13. : Time-structure of the proton bursts from the ISIS synchnotron.

Now this is of vital importance for the muon facilities at ISIS, because the muon beams produced have essentially the same time structure as the ISIS proton beam, ie pulsed at 50 Hz with a double pulse of muons with each pulse ~ 70 ns wide FWHM.

In contrast, the PSI and TRIUMF meson factories are continuous sources with a 20 ns time structure, so that muon facilities at these labs are also continuous.

Such a difference in proton beam time structure is the principal difference between ISIS and meson factories muon sources and affect the experiments which can be done at either in dramatic ways, which we will go into later.

The Pion (Muon) Production Targets at ISIS

All muon facilities are generated from low Z targets inserted in the proton beam. In the ISIS case the targets are thin slabs of pyrolytic graphite (typically 5-10 mm thick in the proton beam direction). Low Z materials are optimal for high pion production and low multiple scattering of the proton beam and hence minimal activation of the downstream proton channel. In the ISIS targets, typically 2 - 3% of the protons interact in the target, while 97% pass unhindered. Hence it is acceptable to generate muon beams all the time ISIS is operational with neutron production: a vital fact considering the need to satisfy a large international muon community. The 10mm targets generate about 1 kw of power requiring edge cooling to these targets as shown in figure (4), which operate typically at ~ 500°C at 200 μA.

Fig. 14. : Photograph of the thin graphite targets used to produce muons. These targets are water-cooled at one edge. Also shown is a profile monitor for the extracted proton beam.

TRIUMF uses similar targets as ISIS, while PSI uses radiative cooled rotating wheels of pyrolytic graphite, targets which in general are much thicker (~ 50 mm) than those at ISIS.

Types of Muon channels

The interaction of the protons in the graphite target at ISIS produces intense pulses of pions born in the reactions discussed previously, with a wide energy spectrum. There are two ways of generating muon beams from these pions. The first and most important is to use low energy pions which actually come to rest in the muon target and which subsequently decay in this target. Because these muons are of low energy (4.1 MeV), the only ones with sufficient range to escape the target are those which stop near or on the surface of the target slab. Hence these muons are known as 'surface' or 'ARIZONA' [23] muons, but as described before, they are 100% polarized in any chosen direction of emission from the target and because of the pion stopping density in the target is very high, then surface muon beams are of high intensity. Another advantage of such beams is that if the proton beam focus at the target is small, then a small source of muons is produced allowing in principal the imaging of this small source to an equally small image at the experiment at the end of the beam-line.

Figure (15) shows how surface muons are produced from pions stopped in the production target.

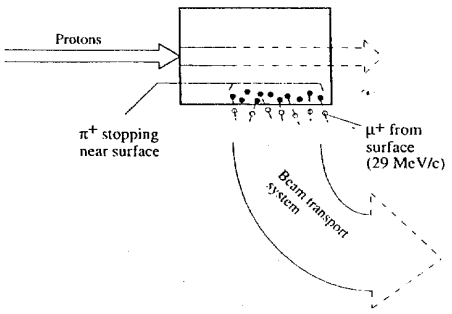

Fig. 15. : Production of surface (or 'Arizona'-type) muons from pions which have been stopped near the surface of the production target.

However a disadvantage of surface muon beams is that they only produce polarized beams of positive μ^+ muons and not of negative μ^- muons. The reason for this is that the potential parents of negative μ^-, ie negative π^- once stopped in the graphite target are immediately captured by the carbon nuclei, their energy is absorbed resulting in a nuclei disintegration or 'pionic star'. Hence the negative pions are lost and cannot be used to create muons in this way. In order to produce negative muons it is necessary to utilize pions which have sufficient energy to escape from the production target, and direct as many as possible into a region of high longitudinal magnetic field where they (or most of them) can decay, producing muons which may subsequently be selected in momentum and transmitted to the experiment. This type of beam line is known as a 'Decay' beam, because pion decay occurs in flight and not at rest, and since nuclear capture does not occur as for a surface beam, this type of channel can produce both polarized μ^+ and μ^- over a wide momentum band. This is indeed the 'Rolls Royce' of muon channels as reflected in the cost £10M compared with ~ £2M for a surface beam.

Polarized Muon Beams from Surface and Decay Channels

It is clear that for surface muon channels, a beam transport system which looks at muons escaping in a particular direction from the surface of the target, must collect muons of 100% polarization and energy of ~ 4 MeV (~ 29 MeV/c momentum). Put another way, in the reference system of the pion (at rest) the muon will be 100% polarized in any direction of emission in the decay. In this sytem the muons are emitted isotropically.

In a decay channel, pions are not at rest and decay while they are passing through a region of strong longitudinal magnetic field, usually provided by a superconducting solenoid metres in length. In this case, one has to refer the decay to the laboratory frame of reference and one should take into account the transverse and longitudinal momentum components of the moving particles. In particular, if one defines a cone or a cylinder of observation, whose axis coincides with the direction of both pion propagation and muon emission, two cases can be distinguished:

i) The muon is emitted in the direction of pion propagation. The momenta p_μ° and p_π of both particles are additive. The muon is emitted in the "forward" direction, i.e. the resultant momentum p_μ is greater than that of the pion from which it originated and has a spin antiparellel to p_μ.

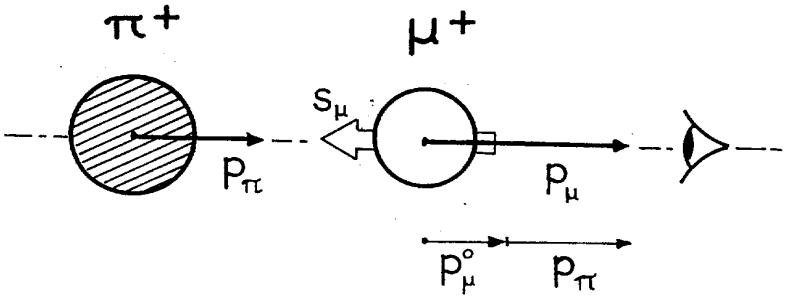

ii) on the other hand, a muon emitted in the opposite direction of pion propagation will carry a resultant momentum p_μ smaller than p_π. Such a "backward" muon will have its spin pointing in the direction of propagation.

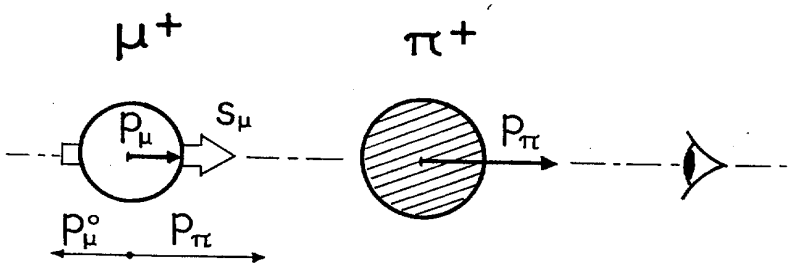

The recipe therefore for obtaining polarized muons either μ^+ or μ^- from a decay channel is therefore quite simple namely.

Choose the momentum of muons required for the experiment and set all the magnets in the muon section of the beamline, to transmit these muons. Select the momentum of the pions into the superconducting solenoid, so that the selected muon momentum corresponds to that for "backward" or "forward" decays of the pions. The required information to do this is shown in figure (16), which displays the forward and backward muon momenta as a function of pion momentum. [24]

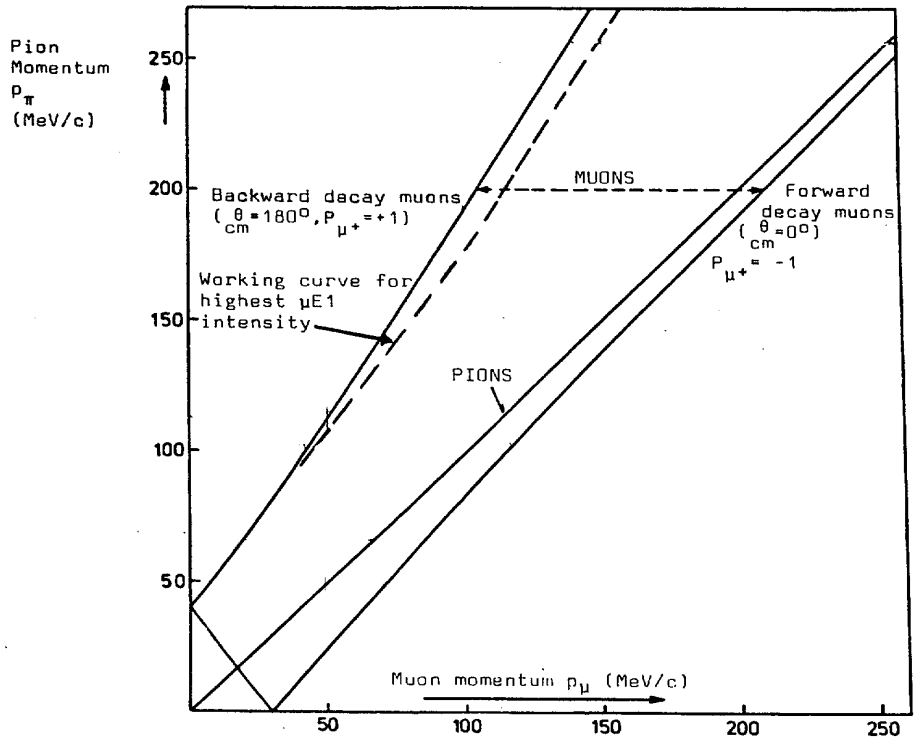

Fig. 16: Decay kinematics for pion decay in flight.

For practical reasons, it is usual to choose "backward" decay muons and as an example if 50 MeV/c such muons are required for the experiment, then from the figure above, one can see that one should inject pions of ~ 112 MeV/c into the superconducting decay section. Such a decay beam produces muon polarization of 70% - 80% due to the finite kinematical acceptance of the channel ie the inability to select only backward decays but a distribution which includes a contamination of non-perfect backward decays. Details of the ISIS RIKEN Decay channel will be described later in these notes.

Transport of Muons to the Experiment

Muons unlike neutrons are charged particles and hence can be deflected in magnetic and electric fields. Magnetic fields in a typical muon beam line are generated and used in quadrupole magnets which are used for focusing the muon beam, and in bending magnets which are used to select a particular momentum for the transmitted muons. Electrostatic fields are used in special devices to deflect the muons appropriately or in combination with magnetic fields. Non relativistically the force on a particle of mass m, velocity v, change e, passing through a magnetic field B perpendicular to its path is given by

Force = Bev in a direction perpendicular to B and v.

The particle executes a circular path of radius R in the field such that

$$Bev = \frac{mv^2}{R}$$

so that the deflection angle is passing through the field ϕ is proportional to $\frac{Be}{mv}$ i.e. proportional to $\frac{1}{P}$.

The magnetic fields required in quadrupoles and bending magnets are proportional to the momentum of the particles concerned.

Similar consideration for electrostatic deflections show that these are proportional to $p\beta$ of the particle concerned. In general deflecting devices based upon electrostatic fields are suitable only for low particle momenta and velocities, higher momentum particles are more efficiently deflected using magnetic fields.

The primary task of a muon beamline is to collect and transmit as many of the muons produced in the target as is possible within the typical aperture constraints of the various elements in the beam-line. A quadrupole magnet if used as a horizontally focusing device is of necessity vertically defocusing and so these must be used in pairs (quadrupole doublet) or in three (triplet) to produce net focusing in both directions.

In a pulsed beam of muons such as the ISIS facility, special care must be taken to remove contaminant particles other than muons in the beam. These are principally positrons in a positive surface muon beam and because their velocity is close to the velocity of light, in contrast to $\beta = 0.24c$ for surface muons, they are readily removable using a crossed magnetic field/electric field separator.

The ISIS Surface Muon Beam (1987 - 1993 [25]

This is shown in Figure (17). The surface muons are collected by the quadrupoles Q1, Q2 close to the target after passage through the thin aluminium window separating the vacuum systems of the muon and proton channels. These muons are momentum analysed in the magnet B1 which is set at the same integrated magnetic field as B2. Q3, Q4 and Q5 produce a dispersed focus of the beam in the middle of Q4, near to which is a horizontal collimator used to select the momentum bite of the beam.

Q7, Q8 transmit the muons through the drift space Q7 - Q8 in which is situated the cross field electrostatic separator A used to eliminate the positrons in the beam. Also in this section of the beam line is a special electrostatic kicker UPPSET which was used to eliminate the second muon pulse. The beam line is completed by a quadrupole doublet Q8, Q9 which produces a simultaneous horizontal and vertical focus of the muons at the sample position in the μSR spectrometer situated at the end of the beam line.

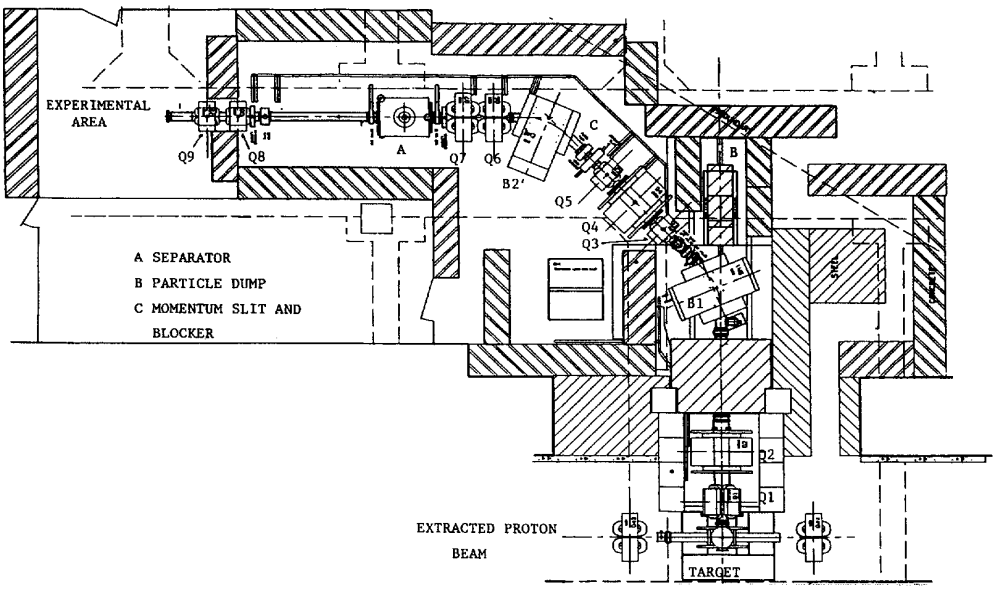

Fig. 17. Layout of the ISIS pulsed muon beam. Muons are produced in thin graphite targets located in the extracted proton beam and collected at a central production angle of 90°. A dispersed focus is produced in the centre of the Q4 quadrupole. Horizontal achromaticity is achieved after the second bending magnet. Positron separation is obtained using the 1 m CERN cross-field separator.

The beam envelopes for this early muon facility are shown in figure (18), illustrating how the quadrupoles are used to transmit the muons with minimal loss from the muon production target to the experimental apparatus.

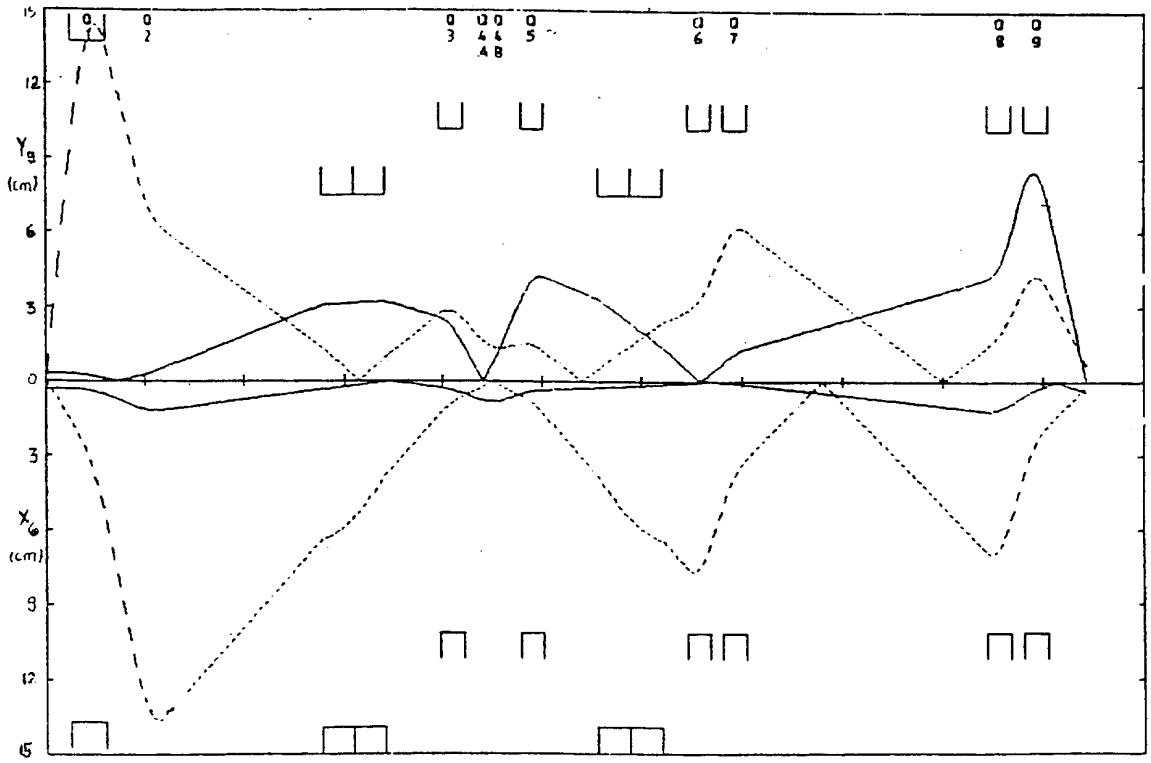

Fig. 18. Principal Trajectories from TRANSPORT for the New Version of the Muon Beam. Trajectories shown are from the centre of the Production Target with Maximal Divergence Y′ and X′, and from the Extremes of the Target with zero Divergence.

Positron Elimination in the ISIS Muon Beam

The muon beam line is set at a surface muon momentum of 26.5 MeV/c transmitting all positively charged particles of this momentum.

Besides the surface muons themselves, positrons exist in the beam line some of which arise from the decay of π^o produced in the target and the subsequent materialization of electron positron pairs in the reactions:

$$\pi^o \rightarrow \gamma\gamma \qquad \gamma \rightarrow e^+e^-$$

Because the π^o lifetime is short (0.83×10^{-16} secs), these positrons are prompt and reflect precisely the time structure of the proton pulses. If all of the positrons were prompt, they would not pose such a serious problem in a pulsed muon facility, however, a sizeable fraction (~ 50%) of the contaminant positrons arise from the decay of muons in the target with a decay time constant of 2.2 μsecs.

The momentum spectrum of positrons from muon decay is shown in the Michel spectrum of Figure (9) where it is clearly evident that many e^+ are produced in this decay at a momentum of 26.5 MeV/c and which we therefore transmitted by the beam line. These must be eliminated in such a beam as they simulate exactly the muon decays in the sample.

This can be done with a cross field electrostatic separator. This is a device which in the ISIS muon beam consists of a vertical electric field between horizontally disposed electrodes, and a horizontal magnetic field generated by anxiliary coils. In such a device, particles of momentum p (GeV/c) and velocity β(v/c) are deviated vertically by an angle Δy′ (mr) given by the expression.

$$\Delta y'(\text{mr}) = \frac{\ell}{p}\left[\frac{\varepsilon_o}{\beta} - 300B\right]$$

ℓ length in m

ε_o Electric field gradient in Mv/m

B field in T

For particles such as surface muons (p = 0.0265 GeV/c, β = 0.24) it can be arranged that $\Delta y' = o$ when $\frac{\varepsilon_o}{\beta} = 300B$. This being the case the muons are transmitted through the device without deviation. For positrons β = 1 and a vertical deviation occurs which for 100Kv applied to the device, is sufficient to remove them from the beam. This device essentially acts as a velocity selector.

Typical values used at ISIS are 100 Kv over the 13 cm gap of the separator cancelled by a magnetic field of 106.9 Gauss. This produces a vertical deviation for positrons of 92mr.

Incidentally this device induces a polarization rotation of the muon given by $\varphi = \frac{eB\ell}{\beta\gamma}$

where e is the charge in the muon and $\gamma = 1/\sqrt{1-\beta^2}$

For 100kv φ = 6.6° at surface momentum pointing upwards from the direction of travel of the muons. Give sufficient electric field gradient and length, π/2 rotation can be achieved resulting in a transformation of longitudinal polarization to transverse. Such a capability is useful for high transverse field experiments and for full flexibility of the facility. Such π/2 rotation would require 454 kv generated over a two cross field separator each 1.5m long.

The continuous muon sources at PSI and TRIUMF do not require the elimination of the contaminant positrons which is obligatory at a pulsed source such as ISIS. The reason for this is that a very thin

scintillation detector placed before the μSR sample can distinguish positrons and muons counted individually by the amount of light they generate in the detector. Positrons are 'minimum ionizing' particles in such a plastic scintillator and therefore can readily be vetoed from the larger light pulse generated by the slower muon.

Provision of Single Muon Pulses using the UPPSET Kicker (1989) [26]

The existence of two muon pulses per acceleration cycle of the ISIS accelerator restricts the magnetic environment in which these muons my be stopped in a sample and hence the research which can be done with these muons.

In an applied transverse magnetic field of 110 Gauss, 330 Gauss etc., it is possible to rotate the polarization of the first muon pulse by 180°, 540° etc. in the time it takes for the second pulse to arrive, resulting in an essentially unpolarized muon ensemble. This being the case no useful μSR measurements can be made at these applied magnetic fields. This is illustrated by Figure (19) which shows the measured μSR transverse asymmetry against applied magnetic field, where clear 'holes' in the μSR sensitivity can be seen at these fields.

In order to overcome this problem, a fast electrostatic (field) kicker was installed in the beam line in 1989, to suspress the second muon pulse. This kicker shown in Figure (20) consists of closely spaced horizontal spaced electrodes, alternately grounded across which an applied HV of ~ 15 kv is generated between the two muon pulses. Muons in the second pulse are kicked vertically by ± 50 mr such that they impinge upon the closely stacked foils of a Soller collimator downstream of the kicker. In this way these muons are prevented from reaching the experiment. Figure 19 shows how this capability removes the inhibiting features of the double pulse structure with a modest applied voltage of 12 kv.

Such operations with single pulses throws away 50% of the available muons. The principle of this method was extended in 1993 with the creation of the European Muon Facility at ISIS, where ε field kicking was used to distribute single muon pulses at 50 Hz simultaneoulsy to three experimental areas.

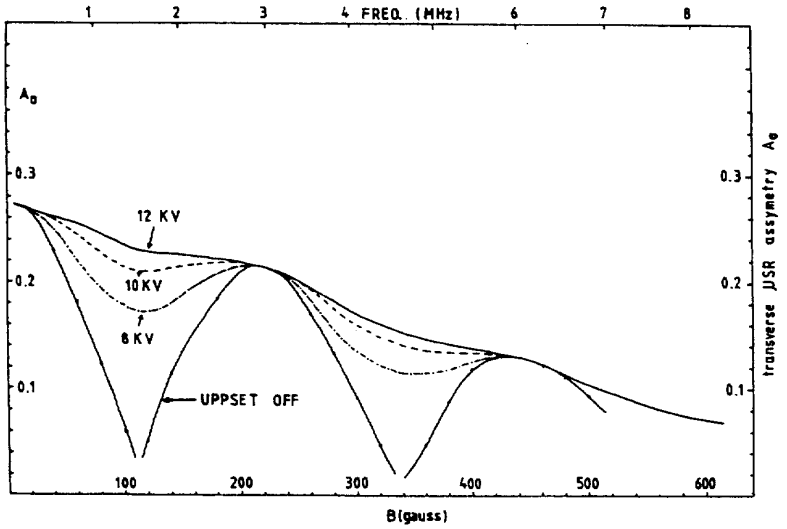

Fig: 19. Dependence of the measured transverse μSR asymmetry from an aluminium sample on applied magnetic field for various operating conditions of the UPPSET device. With the UPPSET device off, the measured response function is a series of peaks with intervening minima close to zero asymmetry. These "holes" in the response function are gradually filled in as the UPPSET voltage is raised in steps to the design voltage of 12 kV.

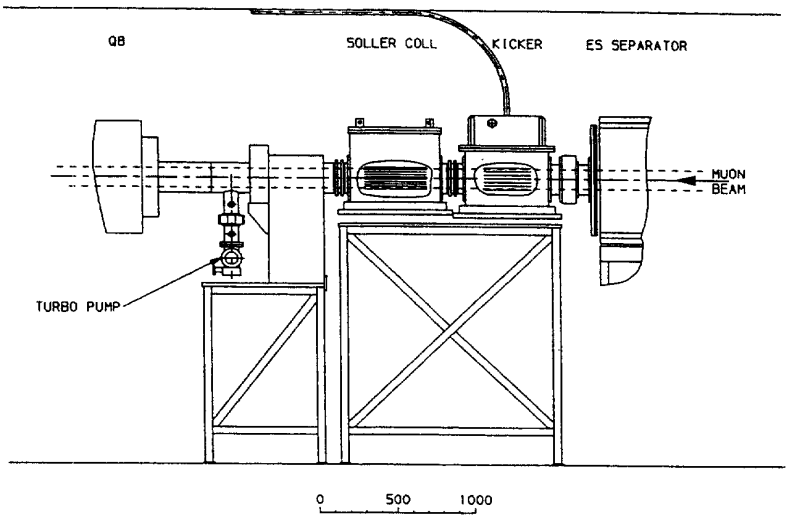

Fig: 20 Side view of the UPPSET system located in the drift space between the cross-field separator and the Q8 quadrupole. The electrostatic kicker is shown relative to the vertical divergence limiting Soller collimator.

The European Muon Facility at ISIS. (1994) [27]

The upgraded EC Muon Facility at ISIS was commissioned in 1994 and provides three areas with simultaneous single muon pulses at 50 Hz. It serves a wide international community of muon scientists and will probably be where you will cut your teeth should you decide after this school to join this community. This facility is shown in the photograph and in figure (21).

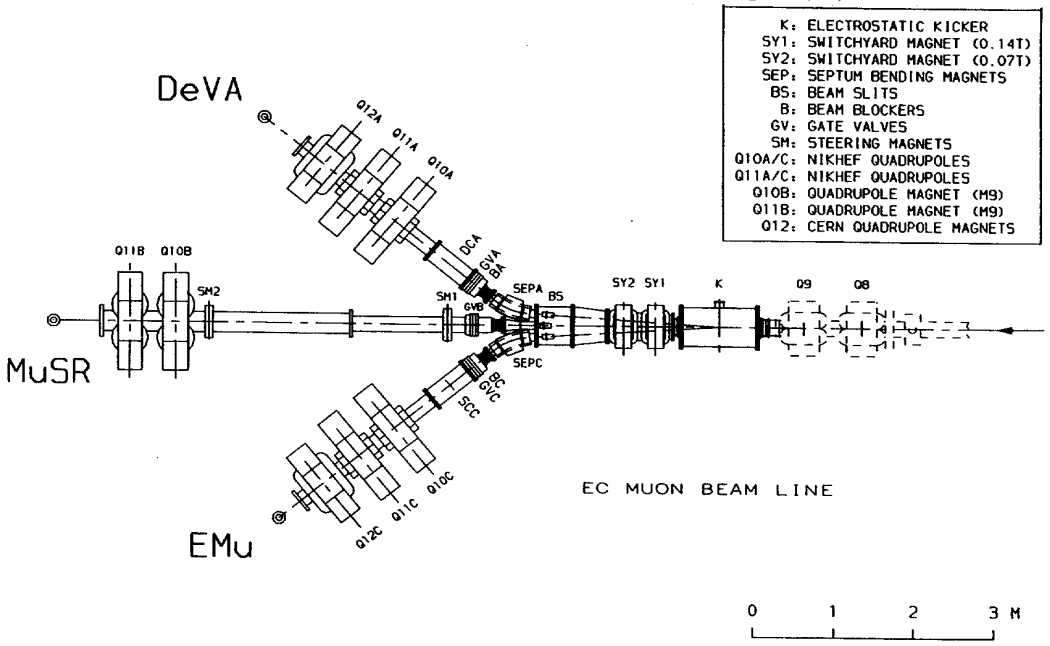

Fig. 21: Layout of the upgraded ISIS muon facility showing the locations of the E-field kicker K, the two septum magnets SEPA and SEPC and the three beamlines.

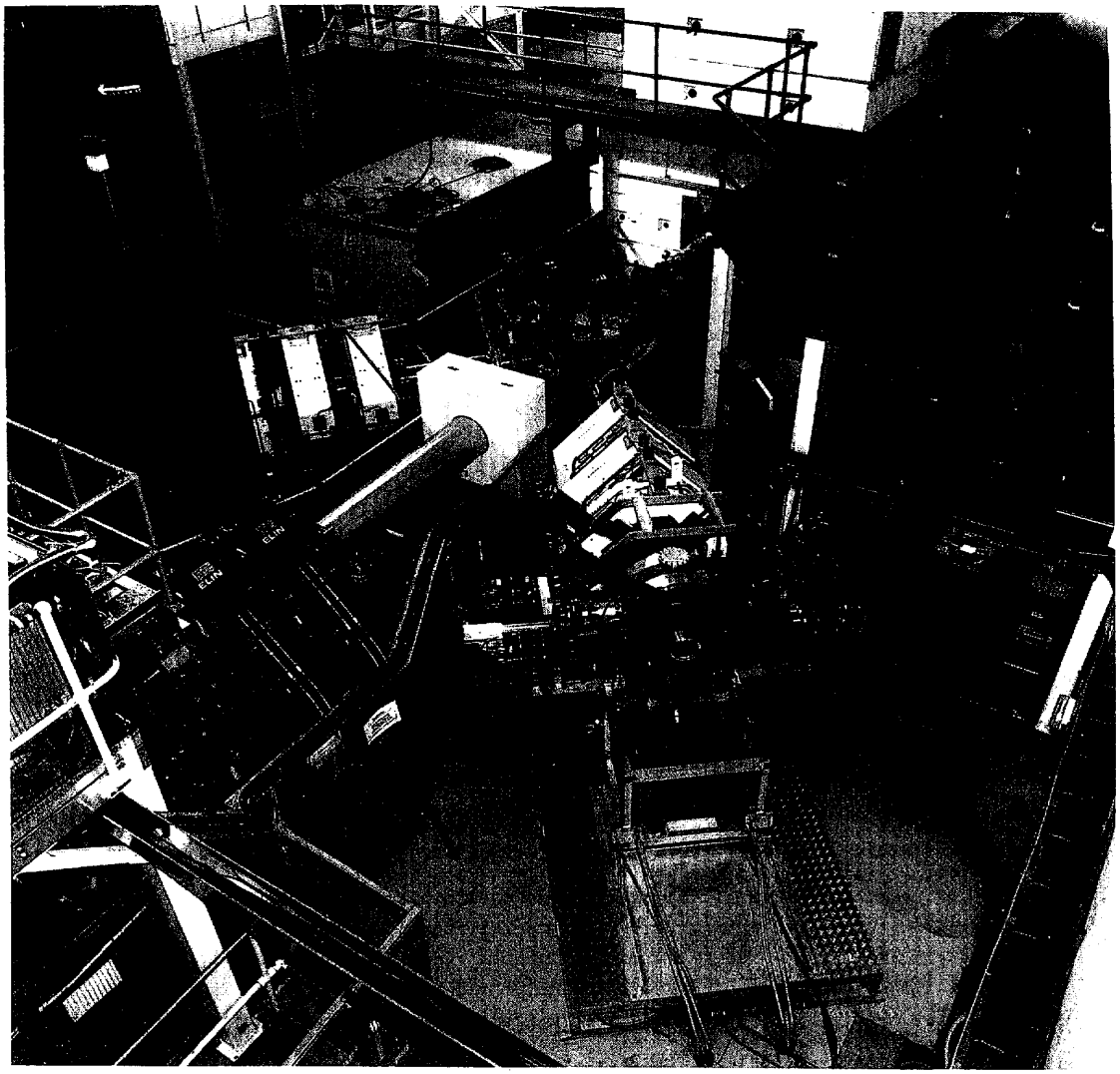

Fig. 22: Photograph of the new upgraded muon facility in the main ISIS experimental hall.

How we manage to create three independent areas with single muon pulses, when we only have two pulses to start with, is done with an electrostatic kicker k shown in figure (21). The layout of this kicker is shown in figure (23), and compared with the UPPSET kicker previously described.

It contains three electrodes, an outer, grounded pair and a thin central anode. The potential of this anode can be reduced from 32 kV to zero in 100ns between the two muon pulses. Therefore, under normal working conditions, the first pulse experiences an electrostatic field on either side of the anode. This gives rise to an equal division of the muon pulse and a right or left deflection of 3.8° to the septum magnet, situated 2.15m downstream of the kicker. Each deflected beam is deviated by a further 36.2° by the septum magnets to produce a total deflection between these beams of 80°. The second muon pulse experiences no electrostatic field and therefore is transmitted through the space between the septum magnets.

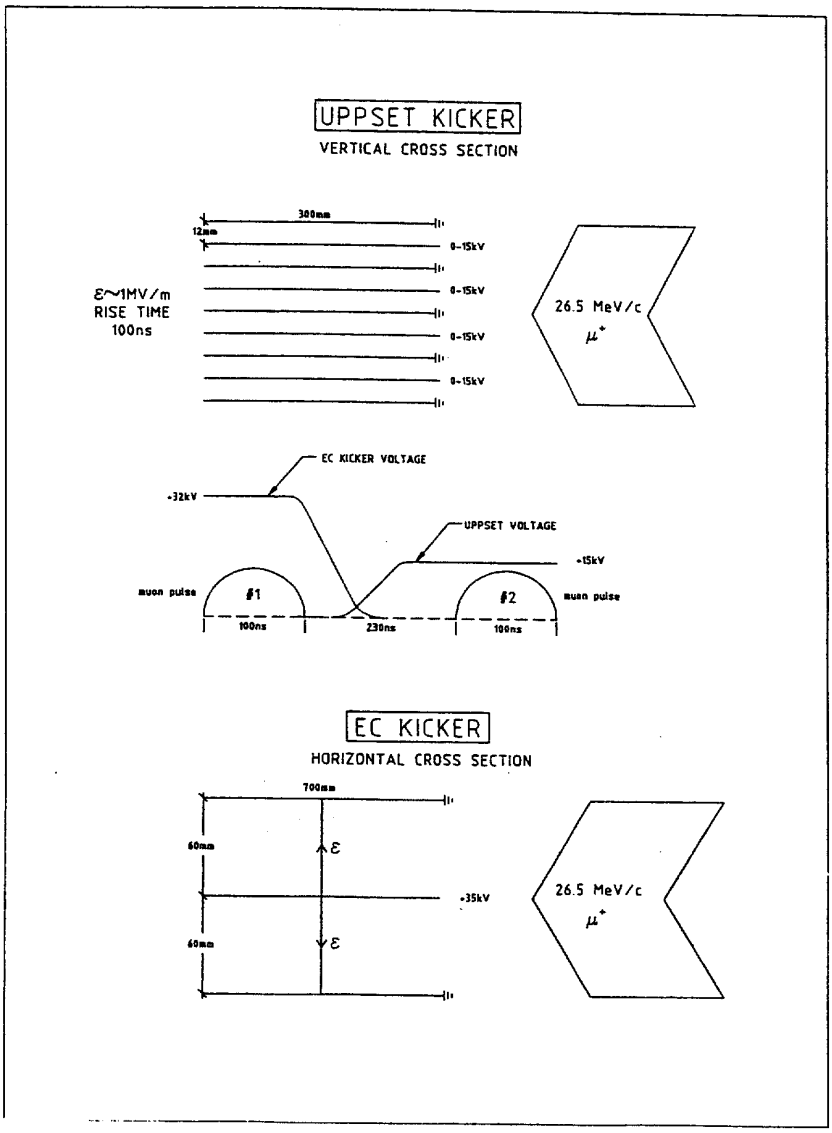

Fig. 23: A comparison between the geometrical layout and voltage waveforms of the UPPSET and CEC E-field kickers shown relative to the incoming muons and the timing of the two muon pulses. The UPPSET voltage (0-15 kV) is shown inverted in the diagram.

The action of this kicker on the original two muon pulses can be seen from figure (24). A little explanation is required to understand this figure. The top trace shows the pulses derived from a Cherenkov counter viewing the muon production target; this detects relativistic particles generated therein and basically gives you the time structure of the two proton pulses arriving at the muon production target. The second and fourth traces show the MUSR and EMU muon pulses derived from scintillator rods mounted in horizontal collimators at the location BS in figure (21). These show a clear separation of the two muon pulses into their septum magnets and hence into their respective experimental areas. A similar pulse (not shown) is transmitted to the DEVA area. The third trace shows the 32.5kV potential on the kicker as it ramps down between muon pulses.

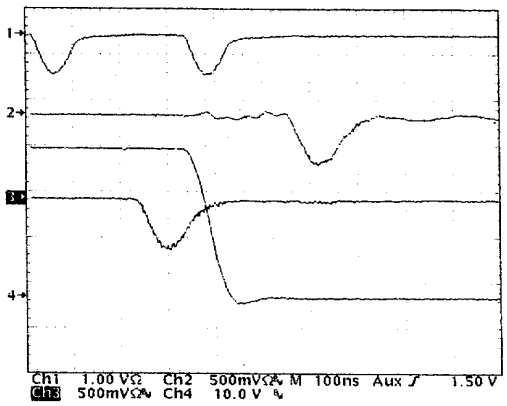

Fig 24: Oscilloscope traces showing the action of the E-field kicker on the double pulses of muons. The top trace shows the Cherenkov pulses revealing the basic time structure of the protons at the production target. The second and fourth traces are derived from the MUSR and EMU collimator counters respectively, showing the action of the kicker wave-form (third trace) in distributing the two muon pulses to the EMU/DEVA and MUSR beamlines.

The three collimators BS allows one to reduce the horizontal muon spot size at the sample for each area and hence optimise the experimental conditions for various size samples, and also allow variation of the counting rate in the experiment.

Performance of the EC Muon Facility

The tables below list various parameters of the MUSR and EMU beamlines and μSR spectrometers.

Summary of measured parameters of MUSR beamline and spectrometer at a ISIS proton current of 180 μA using a 5 mm thick production target, and with a single brass degrader in front of the positron detectors

Horizontal collimator width [mm total]	Spectrometer event rate [10^6 events/h]	Longitudinal μSR asymmetry [a] a_0 [%]	Figure of merit [a_0^2 rate]	Estimated muon spot size (H×V) FWHM [mm]	Percentage of muon [b] spot outside Ø= 24 mm
40	34.2	21.5	15808	15×8	20
30	28.5	21.8(5)	13544	12×8	17
25	24.2	22.7(5)	12470	10×8	13.5
20	20.0	23.4(4)	10950	8×8	13.0
15	15.7	23.7(7)	8818	7×8	12.0

[a] From a sample of $ErAl_2$ masked at Ø 24 mm with silver.
[b] Measured without vacuum window on cryostat.

Summary of Measured Parameters of EMU beamline and spectrometer at a Proton Current of 180 μA using a 5 mm thick production target. (no brass degrader in spectrometer)

Horizontal slit width [mm total]	Spectrometer event rate [10^6 events/h]	Longitudinal μSR asymmetry a_0% [a]	Figure of merit (a_0^2 × rate)	Estimated muon spot size (H×V) FWHM [mm]	Percentage of muons Outside Ø= 24 mm
50	39.2	10.1	3999	27×10	53
40	35.7	12.1	5227	22×10	46
30	28.5	14.4	5909	18×10	36
20	17.2	16.9	4912	10×10	23
10	10.0	18.8	3534	9×10	16

[a] From a sample of $ErAL_2$ masked at ϕ = 24 mm with silver.

Points of interest from these tables include the fact that in both spectrometers one can achieve count rates between 20 - 50 Meg/h. While this may not impress the audience, older researchers will recall in the early days of μSR for example at the CERN SC, one would be very lucky to achieve 1 meg/h and even that had large backgrounds. One can also see final muon spot sizes from 1 - 4 cm^2 variable using the collimators previously mentioned. This is the sort of sample sizes you should bring to ISIS.

Here I should mention a significant advantage of the continuous meson factories with regard to sample sizes. At PSI it is easy to define a small muon spot on the sample, using a scintillation counter with a hole in of the diameter needed, and use this to veto events which register therein. Only muons traversing the hole will be recorded and in this way it is possible to do μSR on samples smaller than easily achievable at ISIS. This technique is possible at PSI because incoming muons are recorded individually, whereas at ISIS, many thousands arrive in each muon pulse. This problem has been overcome to a certain extent at ISIS by the use of 'fly-by' samples. [28]

Hitherto, the standard method used at the ISIS muon facility for mounting samples in the muon beam was to place the sample under study on a standard sample holder and surround it with a suitable masking material such as Haematite (Fe_2O_3) or silver. While this method has been successfully used for many applications it suffers from a number of disadvantages. These are:

The muons stopping in the masking material are detected in their decay with the same efficiency as those stopping in the sample of interest.

The background due to muons stopping in the mask is in some cases temperature dependent and may need to be determined over the whole temperature range of the experiment.

The maximum allowable counting rate determined by early time distortion in the muon decay spectrum is governed by the total counting rate from the sample and the masking material.

Even with the provision of the remote collimation in the muon beam line it is difficult to do experiments with very small samples $\leq 2cm^2$ in area, principally because of two cryostat windows which increase significantly the spot size.

A novel method of irradiating small samples was proposed to overcome these problems. Instead of using a normal masked sample, a transmission sample holder was tested in a transverse μSR experiment. The principle of the method is to place in the vicinity of the muon beam spot, an irradiated sample of the area required ($1cm^2$ in the example shown) supported by narrow arms to the cryostat cold head, where the arms can be sufficiently thick in the beam direction to ensure adequate thermal contact. The arms can be covered with a suitable masking material. Provisions of such a sample holder inside a cryostat, presupposes that the cryostat vacuum vessel and intermediate heat shield are both equipped with thin exit windows to allow the muons which miss the sample to escape from the cryostat and stop some 50 - 60 cm downstream of the sample. At such a stopping location, the counting efficiency for these muon decays will be reduced to negligible proportions compared to the decays in the sample itself.

These ideas have been tested in the MUSR spectrometer with brass samples of the new geometry without any cryostat heat shield and vacuum vessel. It was shown that with a $1cm^2$ brass sample, it is possible to preserve 90% of the transverse μSR asymmetry compared with that for a large unmasked brass sample, while the conventional sample of $1cm^2$ brass masked by Fe_2O_3 gives only 55% of this asymmetry even under the optimised conditions of no cryostat windows. The former asymmetry is weakly dependent on X slit setting, while the latter is, as expected, strongly dependent.

Because of these promising results, the two closed cycle refrigerators (one on MUSR, the other on EMU) will both be equipped with exit windows and a new set of sample plates, to allow μSR experiments with small samples. The method may also be applied to the other cryostats where applicable.

An intriguing extension of this concept is to consider the possibility of collecting the muons which pass the small sample and refocus them downstream with a quadrupole doublet to a second μSR spectrometer.

Experimental Areas of the EC Muon Facility

Three areas MUSR, EMU and DEVA are provided with single muon pulses at 50 Hz with an incident muon momentum from the beam lines of 26.5 MeV/c, (reduced from the full surface momentum by energy loss in various windows).

MUSR and EMU are equipped with dedicated μSR instruments for materials science research, while DEVA is an area where 'exotic' experiments are carried out. These I will describe later. These three areas are complimented at ISIS by the Japanese RIKEN muon facility which is situated on the opposite side of the ISIS extracted proton beam but is fed from the same production target.

The Japanese RIKEN/RAL Muon Facility at ISIS [29, 30]

This will perhaps be described in detail by other speakers, I will only describe this facility briefly. This is shown in figure (25). As described previously, this decay muon channel like all decay channels, has three parts to it which are: a pion injection section near the production target, a 5.5M 5T superconducting solenoid in which the pions of a selected momentum decay into muons, and a muon extraction section which transports the backward decay muons to the experimental area. The pion injector is designed to operate up to a maximum momentum of 250 MeV/c pions and incorporates a pair of large aperature quadrupoles and a bending magnet to maximise the pion rate. The superconducting solenoid produces a longitudinal magnetic field of 5T, which is high enough to capture all decay muons in tight spirals. The decay length λ_π for pions of momentum P_π (MeV/c) is given by:

$$\lambda_\pi = 0.055 \times P_\pi \text{ metres}$$

ie for 100 MeV/c pions λ_π = 5.5M. Ideally it would have been best to have a solenoid ~ 6-7M in length, however this would not have fitted inside the space available, so a compromise of 5.5M magnetic length was reached. Even so this muon facility is by far the most intense source of pulsed muons in the world.

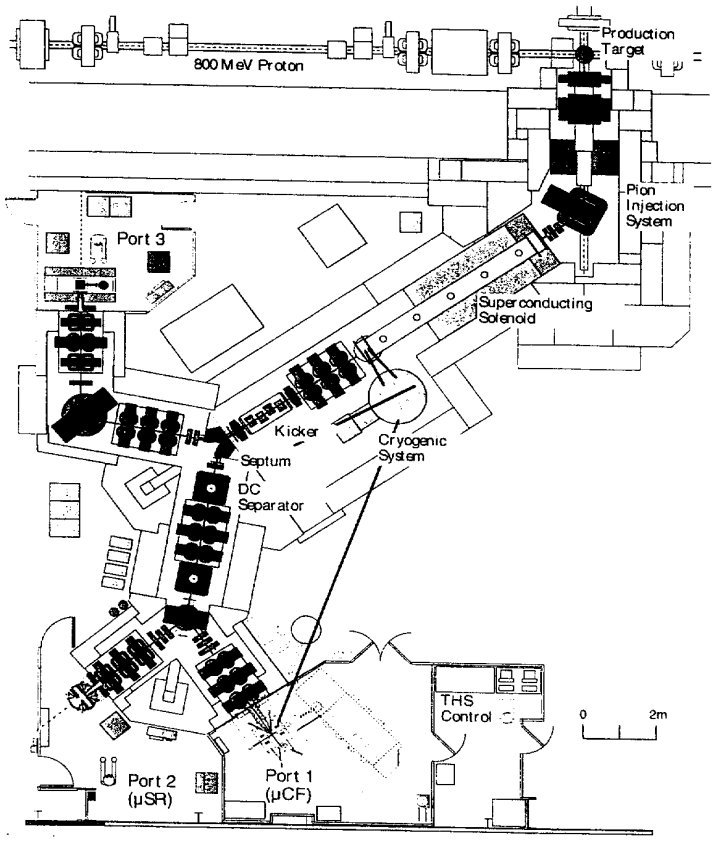

The layout of the beamline and the three experimental ports of the RIKEN-RAL Muon Facility

The exit aperture of the solenoid acts a source of muons, either positive or negative depending on the charge sign of the input pions. The subsequent muon extraction system collects and transports those muons whose momentum corresponds either to forward or backward decays in the pion rest mass. By this method a high muon polarization of (~ 80%) can be achieved.

The muon extraction section has a couple of unique features for a muon decay channel. The first is a fast magnetic kicker shown in figure (25), which rises in magnetic field (to 0.02Tm) between the two muon pulses. In this way it is capable of separating these two muon pulses into two septum magnets and two beam lines, so that two experimental areas can receive single muon pulses at 50 Hz, like we do on the EC muon facility. The separation is possible up to a maximum muon momentum P_μ = 55 MeV/c, above this and up to 120 MeV/c P_μ, both pulses are directed to any one of the two beamlines with steering magnets. The northward beam (to bottom of fig (25)), incorporates a switch yard magnet so that muons can be delivered to Port 1 or Port 2 for experimental use in either of these ports.

This beamline incorporates two cross field electrostatic separators which eliminate the positron background in Port 1 or 2.

Experimental Areas of the RIKEN-RAL Muon Facility

Port 1 of this facility is equipped with a highly sophisticated apparatus for research in muon catalysed nuclear fusion. This is a dedicated experiment which will be used over many years and which is already producing world class data of unprecedented quality. The permanence of this equipment, the high rates and very small backgrounds offers unique opportunities in this research field.

Port 2 is the RIKEN μSR facility designated ARGUS, in which surface muons are used. Such use requires the whole beam line to be tuned to surface momentum - 28 MeV/c, and the design of the spectrometer allows unprecedented data acquisition rates approaching 100 Million events/hour.

Port 3 is a general area for users to bring special apparatus for short (~ months) stays, and is presently fully occupied with Japanese research on muonium production from hot foils and laser transitions in muonium.

Conclusion

ISIS now offers to the muon community, a complex of muon beams similar in number to those at PSI and TRIUMF, with the unique features afforded by the pulsed nature of the source. These advantages have not yet been pointed out in detail, I will deal with these points later in the instrumentation section of these notes. The pulsed source at ISIS is complementary to the continuous sources, so it could well be that future users like our present community will work at both types of sources, utilising the advantages of both as required.

The TRIUMF and PSI sources I believe will be described by other speakers, but for completness I show the layout of beam lines at PSI in figure (26).

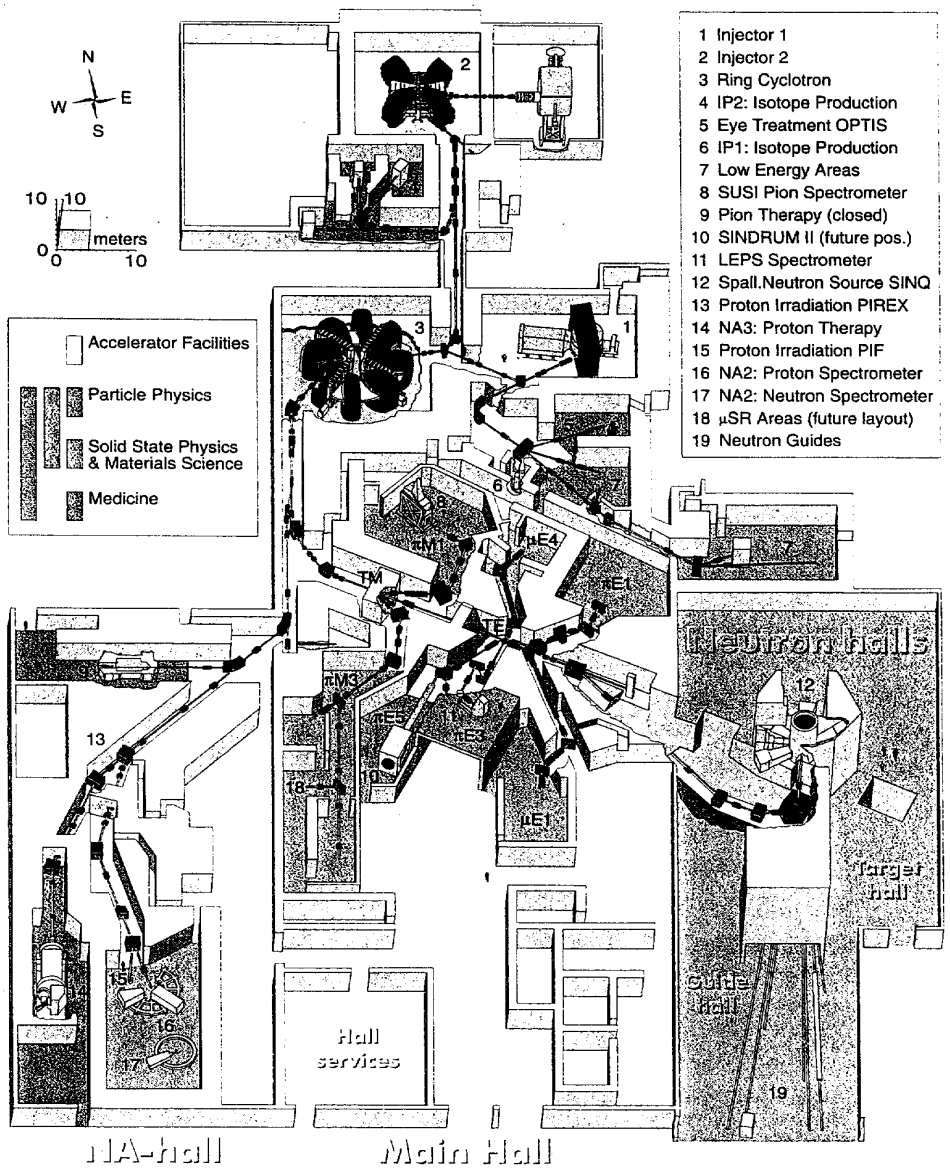

PSI offers two decay muon beams and two surface muon beams dedicated to μSR research in material source. The decay beams μE1 and μE4 can be seen in the figure, together with the surface beams πM3 and πE3. Two target stations TM and TE are used to produce these beamlines.

TRIUMF offers a similar complex of muon facilities, I refer to other speakers for details of these.

Muon Experiments and Instrumentation

Introduction

Up to now we have discussed how to produce muon beams; now we come to the fundamental question namely, what are muons good for and why we use all here to discuss there virtue, if any. Well it will be clear that indeed muons have many virtues, some quite miraculous. To me it would indeed be a miracle that because the muon has the mass which it has, then the worlds energy problems could possibly be solved for the next millennium at least, but I will return to this intriguing point later. Let us start with the best known use of muons namely in probing the properties of materials using the techniques of Muon Spin Rotation, Relaxation and Resonance, subjects in which most of our students in the last decade have got their Ph.d's.

Lets review the most important feature of muons which allow us to use them in μSR.

These are:

Muons are produced fully or almost fully polarized, ie their spins are all in the same direction.

In slowing them down in a material, this polarization is fully preserved.

Muons being leptons do not interact strongly with anything, they only experience the weak and electromagnetic forces. Hence a stopped muon will sit minding its own business in a material until it decides to decay. However much it tries to mind its own business, because the muon has a magnetic moment, if magnetic fields are present at the stopping site, the muon spin will precess around the magnetic field at a frequency which depends on the field experienced. The oft-used analogy is that the muon is therefore a microscopic gauss meter, telling us what the magnetic field is in the material.

However it can only do this because the emitted positron at the moment of decay prefers to travel in the direction of the muon spin. The emitted positrons act like a searchlight rotating at the same frequency as the muon spins in the sample and hence by detecting this searchlight, we can directly measure the rotation frequency of the muons in the sample, and hence the internal magnetic fields. This basically is the principle of Muon Spin Rotation.

Instrumentation for μSR Experiments

Transverse Field time Differential μSR. (TFμSR)

The simplest apparatus for transverse field μSR is that used on a continuous source. An example of such equipment is shown in Figure (27).

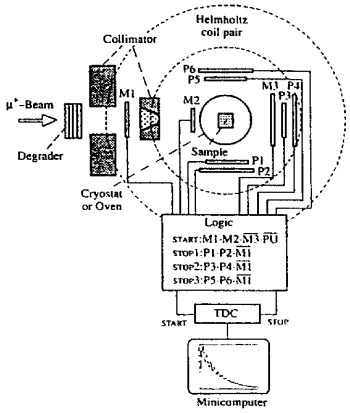

Fig. 27: Apparatus for transverse field time differential μSR on a continuous muon source. The magnetic field is perpendicular to the detector plane and to the incoming muon polarization.

In this apparatus, individual muons enter the apparatus from the left, are degraded in energy in a degrader, and pass through a thin scintillator detector M1 which times the arrival of the muon to the sample. A pair of Helmholtz coils provide a magnetic field transverse to the initial muon polarization (which we remember points backwards). Scintillation detectors are arranged in a box configuration around the sample in a box configuration around the sample in a plane perpendicular to the applied magnetic field. The time difference between a detected positron and the arrival time of the muon is measured electronically and displayed in a computer. In the example shown positrons have to pass through two detectors eg P5 and P6 to be registered. Events in any such double counter, accumulated over many incident muons (say 1 million) have a time distribution relative to the incident muon, which shows the characteristic 2.2 μsec muon lifetime, modulated by wiggles in the spectrum caused by the rotating muon spin. Such a spectrum is shown in Figure (28), the famous μSR spectrum beloved by all muon physicists.

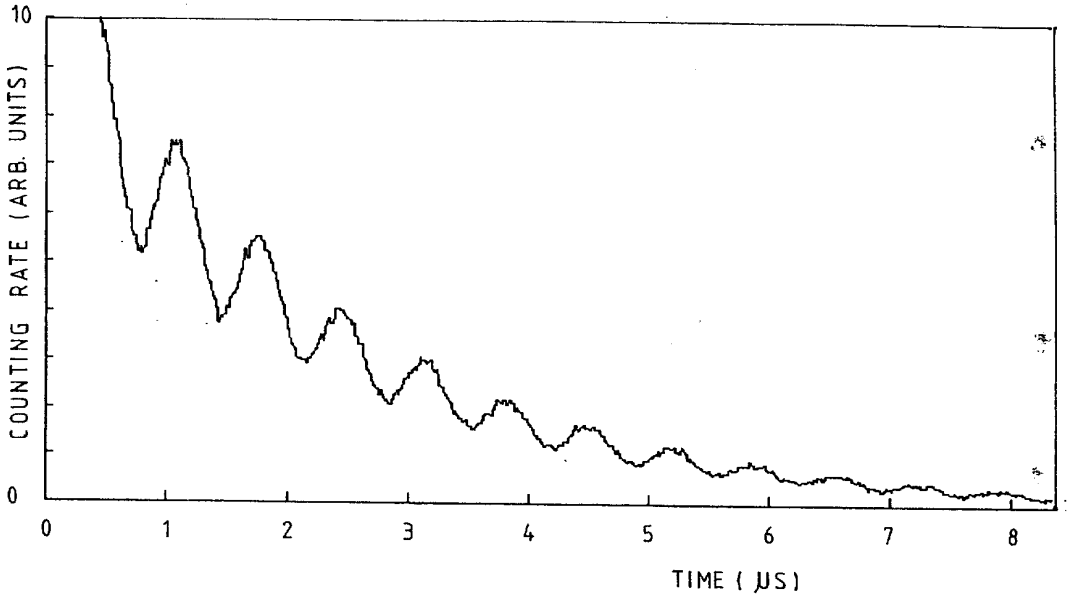

Fig. 28: Time Spectrum of events detected in transverse counters relative to the arrival time of the muon at the sample. The spectrum shows the 2.2 μsec muon life exponential with a modulation arising from the muon spin precession in the sample.

The modulation frequency in this spectrum is that of the muon spin in the magnetic field experienced at the muon stopping point in the sample. This frequency is given by the muon gyromagnetic ratio

$$\gamma_\mu = 13.55 \times 10^3 \quad \text{Hz / Gauss.}$$

ie at 200 Gauss, the observed oscillation frequency is 2.7 MHz. Hence using this technique one can measure the internal magnetic field of the sample and this has wide repercussions in the study of magnetic materials, superconductors etc., which will be covered by other speakers.

In the context of transverse field time differential μSR, it is instructive at this point to contrast the relative virtues of continuous and pulsed muon sources for this sort of work.

Transverse Field time differential μSR at continuous sources

As described before, in the apparatus of Figure (27), single incoming muons are introduced to the sample, and the decay of this muon is detected. This has to be done before the next muon arrives

otherwise one cannot distinguish which muon has decayed. In such a conventional μSR experiment, this is a serious disadvantage of a continuous source, because in these circumstances one has to limit the beam intensity to ~ 5 10^4 muon/sec, so that the probability of a second muon arriving during a time interval of say 10 μsecs is negligible.

Since most continuous muon sources provide ~ 10^6 muons/sec, severe collimation has to be used to reduce the beam intensity to acceptable levels on the sample, and hence typically only a few per cent of the available muons can be used.

This restriction can be removed in time-integral experiments when one is not interested in details of the time distribution of the decay muons. In this case all of the available muons can be used. This point will be covered later.

A further disadvantage of continuous muon sources for time differential transverse μSR is the question of the time window available for the experiments. Because the source is continuous, the experimental backgrounds at the positron detectors becomes significant after a couple of muon lifetimes (~ 5 μsecs), so normally a spectrum such as shown in figure (28) is limited to a time window of 0 - 5 μsecs. As we will see later this is not true of similar experiments performed at a pulsed source such as ISIS, where spectra can be observed up to 30 μsecs (15 muon lifetimes).

On the other side of the coin, for time differential μSR measurements, continuous sources have a significant advantage over a pulsed source, and this is related to the time resolution possible in either case. At a continuous source, the time resolution is limited only by that of the individual detectors giving the START and STOP signals for each event, and this is typically fractions of a nanosecond. Hence μSR frequencies up to and beyond 100 MHz are detectable. At a pulsed source such as ISIS, the time width of the muon pulse (~ 80 ns FWHM) limits observable frequencies to 8MHz or so in conventional μSR experiments. This however can be extended using special RF techniques which I will refer to later.

Transverse Field Differential μSR at Pulsed Sources

The apparatus shown in figure (27), has to be dramatically changed in order to do μSR experiments on pulsed sources. This can be seen from figure (29) which shows the DIZITAL μSR instrument in the MuSR beam at ISIS.

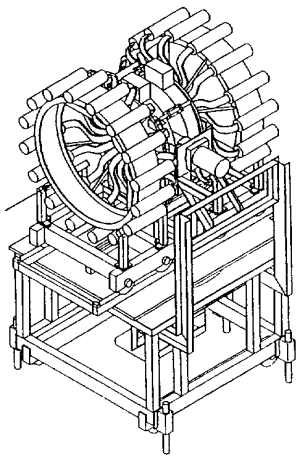

Fig. 29: Example of a multidetector set-up for μSR: the DIZITAL spectrometer at ISIS (Rutherford Appleton Laboratory). It has 16 forward and 16 backward detectors in the longitudinal configuration shown. Helmholz coils produce a magnetic field along the cylindrical axis (arrow). It can also be used for transverse-field measurements.

This instrument requires segmentation of the detectors counting the muon decays because in contrast to continuous sources, where one muon is introduced at a time, on ISIS, thousands of muons are introduced per pulse (typically 10,000/pulse on MuSR), and these all decay with a meanlife $\tau_\mu = 2.2\mu$secs. This is equivalent to a total counting rate of $\sim 5\ 10^9$/sec (5 GigaHerz). Hence in order to handle this sort of rate, segmentation of the detectors is required 32 detectors on MuSR, 100 detectors on RIKEN-ARGUS. Once this is done however, the spectrometer can handle all the muons thrown in at 10^4 muons/pulse at 50 Hz. Therefore μSR experiments at pulsed sources are in general much faster than conventional time differential ones on continuous sources.

As remarked before, another great advantage of pulsed sources, is that once the muon pulse is introduced into the sample, the ISIS accelerator goes to sleep for 20 μsecs, before the next acceleration cycle. This means that during the μ decay, the backgrounds at the experiment are very low so that muon decays can be traced over many muon lifetimes, even up to 15 lifetimes, as shown in figure (30).

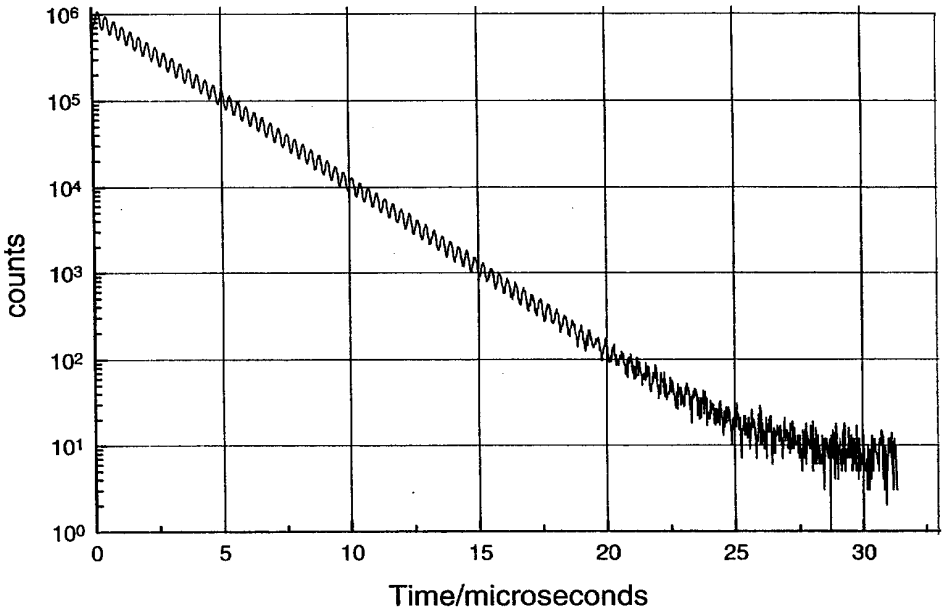

Fig. 30: Typical μSR transverse field spectrum at ISIS (2.2 μsecs exponential removed) showing ability to trace muon behaviour up to 15 τ_μ.

Longitudinal Set-up for μSR experiments (LF μSR, ZF μSR)

An alternative method to transverse field μSR is the situation where the muon polarization is not rotated in a transverse magnetic field, but where the apparatus and any applied magnetic field is longitudinal to the muon polarization. Such as (LFμSR) scheme at a continuous source is shown in figure (31).

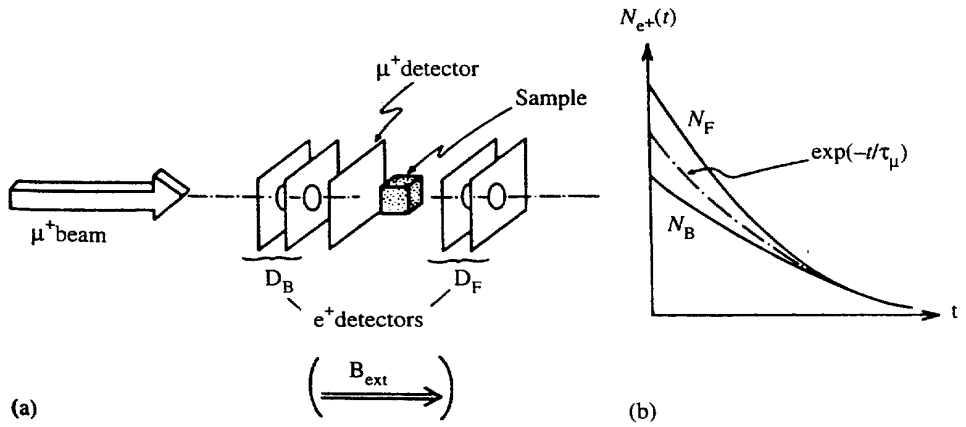

Fig. 31: (a) Experimental Arrangement for longitudinal field (or zero field) μSR. (b) Counting rates observed in forward and backward counters for a sample in which the muon polarization decays and hence the curves approach the experimental 2.2 μsecs decay function characteristic of muon decay.

In this arrangement, positron detectors are placed upstream and downstream of the sample in the direction of the incoming muons (and their polarization). Holes are provided in the backward counters to let the muons in; similar holes are also provided in the forward counters to give the same solid angle acceptance.

Because the muons are initially polarized forwards (from a decay muon beam accepting backward decays see page 16), the forward counters in figure (31) initial count more muon decays than the backward counters as shown in Figure (35) b. However if the muon polarization decreases with time, ie relaxes, due to the interaction of the muon spins with random magnetic fields from surrounding nuclear or ionic dipoles in the sample, then these two counting rates N_F and N_B approach each other as a function of time. The term used in such experiments is the forward/backward asymmetry in counting rates relaxing due to a gradual muon depolarization.

Such experiments can even be done with no applied longitudinal field, in a set up known as zerofield (ZF μSR). Here the earths magnetic field at the sample has to be carefully compensated by sets of auxiliary coils.

All three techniques (TFμSR, LFμSR and ZFμSR) are used extensively in μSR experiments at the worldwide muon sources. In addition some specialized techniques for specific purposes have been developed over the years. These include stroboscopic methods mainly used for measurements of small magnetic shifts, the observation of level crossings in systems with several interacting spins and more recently the use of resonant RF fields, which are particularly suited to pulsed sources. I will briefly refer to this later in the report.

μSR Instrumentation at ISIS

The μSR spectrometer DIZITAL in the MuSR area of ISIS is shown in Figure (29). This instrument is rotatable about a vertical axis, so that it can be used in both transverse and longitudinal geometry. Auxiliary coils are attached to allow zerofield measurements. The μSR instrument in the EMU area is similar to DIZITAL but is fixed in longitudinal geometry. This instrument is shown in figure (32).

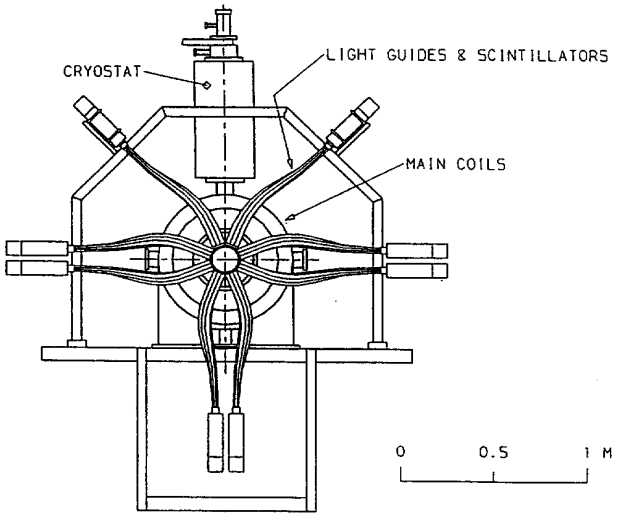

EMU

Fig. 32: The EMU μSR spectrometer at ISIS. Muons enter the apparatus perpendicular to the page.

The technical specification for these two instruments are shown in the table below.

Technical Specification for MuSR and EMU (revised 1996)

Beam

Production target	5, 7 or 10 mm graphite
Momentum of μ^+	26.5 MeV/c, 10% momentum bite
Pulse structure	single pulse 80 ns FWHM
Contamination	$e^+/\mu^+ < 0.015$ (separator voltage> 70 kV)
Beam size at focus (FWHM)	vertical 8 mm (MuSR), 10 mm (EMU) horizontal, adjustable 7 - 15 mm (MuSR) 10 - 27 mm (EMU)
Total intensity	4×10^5 μ^+/s shared by the three areas (5 mm target, ISIS current 180μA)
Polarisation	100%
Range	approx. 110 mg/cm^2
Background	Histograms contain a constant background of about 10^{-5} times the count in the first bins
Data acquisition	Both instruments have 32 TDCs with time resolution settings of 8, 16, 24 or 32 ns and each instrument is controlled by a VAX station 3200.

Sample Environment

MuSR	Helmholtz coils (0 - 200 mT) (transverse or longitudinal) Zero field compensation (<3μT) Closed cycle refrigerator (12 - 340 K) Orange cryostat (2 - 300 K) Dilution refrigerator (40 mK - 4.2 K)
EMU	Helmholtz coils (0 - 450 mT) (longitudinal only) Calibration coils (0 - 10mT) (transverse) Zero field compensation (< 3μT) Closed cycle refrigerator (12 - 340 K) Oxford instruments cryostat (2 - 300 K) Sorption cryostat (350mK - 300 K)

A few technical points concerning μSR experiments

Muon Range and Range Straggling

When implanting muons into a sample, consideration is required concerning the stopping range of muons from surface or decay muon beams. This range R also has a range width or straggling ΔR, arising from the statistical nature of the energy loss before stopping and also due to the momentum spread of the muons themselves.

R and ΔR are given by the following expressions

$$R = ap^{3,5}$$

$$\Delta R_{TOF} = a\left[0.008 + 12.25\left(\frac{\Delta P\mu}{P\mu}\right)^2\right]^{0,5} p^{3.5} \text{ where p = muon momentum in MeV / c}$$

In EMU and MuSR, with surface muons of 26.5 MeV/c, R is typically 110mg/cm^2 and ΔR = 20% of R. The range is therefore about 1 mm, ie the muons stop in the bulk material and not on the surface.

Decay beams of high momentum P, allow much longer ranges and hence the use of sample containers with thick walls, such as pressure cells.

Dead Time of the Detection Systems

The time at which a muon decays into a positron is completely random so the interval between the pulses from the discriminator varies widely. Because various parts of the detector have limitations on the speed with which they can respond this leads to a failure to record two positrons as separate events if the interval between their arrival in the detector is too small.

There is a "dead time" after each event and the observed rate of positron decays will be less than the true rate obtained for a system with negligible dead time. This is a well known problem in particle physics and a detailed treatment can be found in standard textbooks [32]. The simplest case is when for a true rate, r, there is no response at all for a time r_d after each pulse but perfect recovery after this interval. In the literature this is called a non-extendible dead time (or alternatively the non-paralysable case). Then the observed rate is:

$$r_{ob} = r / (1 + rr_d)$$
$$r = r_{ob} / (1 - r_{ob} r_d).$$

There are other models showing dead time effects and in real systems it is often difficult to decide on an appropriate one. However in the MuSR and EMU instruments we find experimentally that the distortion is typically 5% at the beginning of the histogram i.e. $r_{ob}r_d \approx 0.05$ and the equation above is adequate to correct the data.

Muon Science Experiments suited to Pulsed Sources

There are many experiments in muon science which either benefit in varying degrees from the pulsed nature of the source or indeed depend upon it. Many of these research topics are currently underway at ISIS and will be developed in future facilities. This section of the talk is included to enthuse the audience for the exciting possibilities of the near future; many of these points will be covered in detail by other speakers so brevity will be my guiding principle. A few of the points to be covered are the following:

Radiofrequency techniques with Muons.

Studies of muon catalyzed nuclear fusion.

Fundamental Physics Studies with Muonium using pulsed lasers.

Studies in material science using ultra slow muons.

RF Techniques with Muons

The possibility of adopting magnetic resonance methods for use with muons has long been realised. Indeed, in 1958, only a year after the birth of the subject in a paper by Garwin et al [16], Coffin et al (1958) [33] demonstrated the use of radio-frequency (RF) excitation in a μSR experiment. However, perhaps because of the short lifetime of the muon or, more probably, because of the simplicity and success of the rotation and relaxation techniques, the general use of resonance methods has not occurred. Nevertheless, following the impressive study of RF techniques at KEK [34], a limited number of groups have used resonance methods to investigate topics including chemical reactions [35], final state determination [36, 37], Iron [38] and semiconductors [39, 40].

When working at a pulsed muon source such as ISIS the motivation for developing resonance techniques is high. At a continuous muon source the maximum muon precession frequency that can be observed in a transverse experiment is restricted only by the time resolution of the detectors. This is not the case at a pulsed source where the maximum observable frequency is instead limited by the width of the muon pulse (the ISIS muon pulse width of 80 ns corresponds to a maximum usable frequency of approximately 6MHz). Resonance techniques provide a method by which this restriction can be completely removed. Furthermore, for reasons that will be discussed below, resonance experiments are especially suitable for implementation at pulsed muon beams.

Because of the short lifetime of the muon, the application of resonance techniques demand the generation of strong RF fields that, depending on the sample size and coil design, can require RF power levels of up to 2kW. At continuous muon sources the RF duty cycle can be as high as 50% [37] with consequent experimental problems because of RF heating effects. Kitaoka et al (1982) [34] have pointed out that this difficulty can easily be removed at a pulsed muon source where, by timing the RF field to be coincident with the muon pulse, a low duty cycle can be achieved. In fact at ISIS, triggering a 20μs RF pulse every 20ms at each muon pulse gives a duty cycle of 0.1%. This low duty cycle does particularly benefit the implementation of the 90° pulse method proposed at ISIS [41], where very large RF power levels are necessary to achieve the required sub-microsecond RF pulses.

An impressive example of how the 90° pulse method can be used to overcome the normal limit in frequency response of a pulsed muon source, is that from the recent work of Cottrell et al [42] at ISIS. Using longitudinal geometry with an additional counter parallel to the initial muon polarization, a 300ns long pulse of 23.5MHz RF was applied perpendicular to the static field of 17.2G, resulting in a 90° precession of the muon polarization. The subsequent transverse field spectrum shown below was obtained for muonium in quartz.

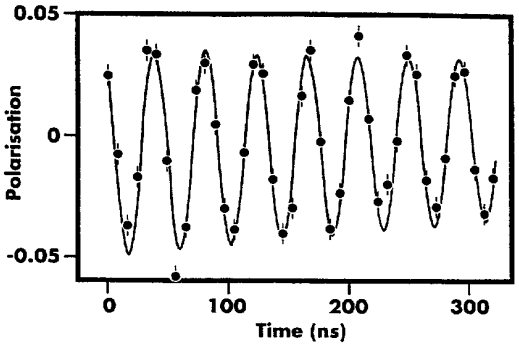

Fig. 33: Free precession of muonium in quartz following a 90° RF pulse at 23.5 MHz.

This observed frequently is well beyond that normally observable at ISIS using established μSR techniques and is a promising development project current at the DEVA muon facility.

Working at a pulsed muon source brings two additional advantages. Firstly, since all data collection is inherently time differential no experimental time penalty is involved in analysing data in this manner and secondly, because of the very low background between muon pulses, data can be measured to long times.

Further development of this technique at ISIS and future accelerators could benefit from this abandonment of digital counting techniques used hitherto and use of analogue detection systems pioneered at KEK by Yamazaki [43] and already demonstrated at ISIS by the Stuttgart and Munich groups [44].

Studies of Muon Catalysed Nuclear Fusion

This subject is one of the most fascinating and exciting fields of research using low energy muons, this is my own personal view, shared by many. For those not familiar with the subject, I refer to an excellent review article [45].

Following on from pioneering studies at KEK, PSI, TRIUMF and Los Alamos, the Japanese RIKEN group established a new collaborative muon facility at ISIS, to be used predominantly for muon catalysed fusion research. This facility has now been operating for four years and data of unprecedented quality is now being produced [46]. I will leave detailed reports on this to Professor Nagamine, but merely show the x-ray spectrum from μ catalysed fusion in DT mixtures in figure (34), which clearly shows the K_α and K_β lines from μ He^4 sticking in the nuclear fusion process, one of the key features which has to be understood if such a process will ever have repercussions for energy productions in the future.

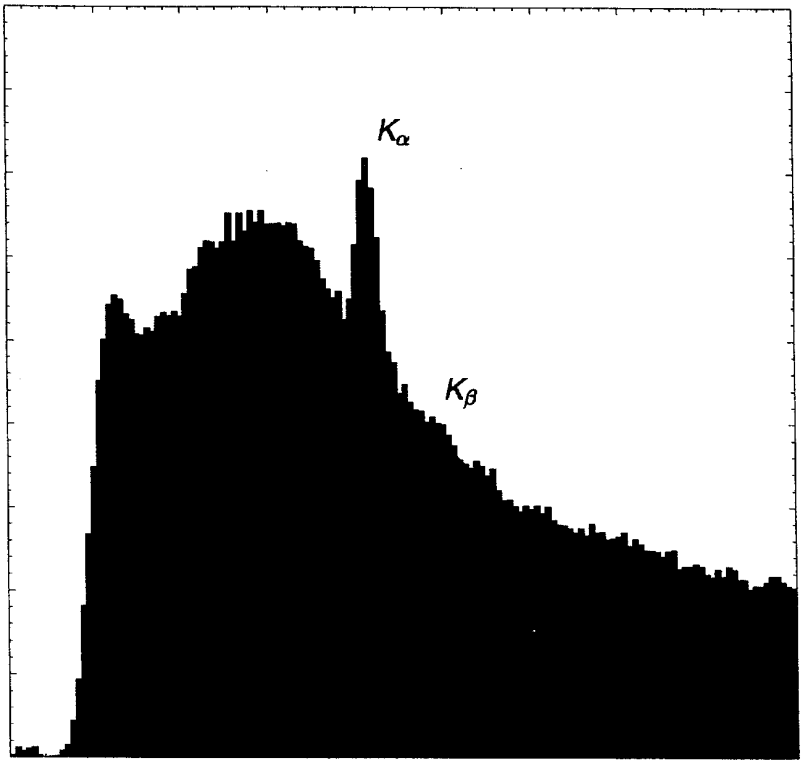

Fig. 34: X-ray spectrum from μ catalysed nuclear fusion in DT mixture obtained by the RIKEN group at ISIS. The K_α and K_β from μ He^4 sticking can clearly be observed.

These μCF experiments benefit at a pulsed source, principally from the very low backgrounds after the muon implantation in the sample, as clearly seen from figure (34), where it would have been difficult if not impossible to have observed the μHe^4 signature with continuous beams of muons.

Fundamental Physics Studies with Muonium using pulsed Lasers

There is a whole class of experiments which need a pulsed environment in time with the muon arrival, which can only be done on pulsed muon sources. Such a pulsed environment include high pressure pulsing, the short term generation of ultra-high magnetic fields or pulsed irradiation with high intensity laser light.

An example of the last type of experiment is the Heidelberg/Oxford/RAL/Sussex/Yale Collaboration's recent work on muonium at ISIS.

Muonium consists of a positive muon with an orbiting electron and since the muon is a lepton with no internal structure (down to dimensions 10^{18}m), it provides a perfect atomic system for precise tests of bound-state quantum electrodynamics (QED).

The experiment [47, 48] measures the 1s - 2s energy splitting using Doppler free two photon laser spectroscopy, incorporating a high power pulsed laser system in time with the arrival of the muon pulse. This experiment has measured the 1s - 2s transition frequency to an unprecedented level which agrees with QED predictions. Recent runs will further improve the precision.

Ultra-Slow Muons as a μSR probe for Surface and thin Films

As pointed out before, surface muons have a range of about 1 mm in materials, hence these cannot be used for probing the properties of surfaces or very thin films. For example, 4 MeV muons have a

range and range spread in silicon of 150 and 20 mg cm^2 corresponding to 710 and 100 μm respectively. To probe surface thicknesses of ≤ 100 nm, requires polarized muons of kinetic energy of ~ 10 KeV and in reasonable numbers.

The table below shows range data for low energy muons.

Range and Range Spread of Low Energy Muons in Silicon

Kinetic Energy E(KeV)[ev]	Range R(nm)	Range Spread ΔR (nm)
0.010[10]	0.5	0.3
0.100[100]	2.1	1.3
1.0 [1000]	13.1	5.4
10.0 [10,000]	75.0	18.0
30.0 [30,000]	244.0	36.0
4,000 Surface	710,000	100,000

The recent development work at PSI [50] of the moderation technique first demonstrated at TRIUMF [49] has shown that for a fully polarized surface muon beam incident on an aluminium substrate and a solid layer of a rare gas or nitrogen, approximately 10^{-4} of these muons emerge from the back face (the solid noble gas) with energies peaked at 10eV and a polarization of 87+3% and 80±20% in the respective cases of Ar and Kr layers used as the moderator. These results indicate that the moderation process is fast compared to any depolarization mechanisms and that this technique satisfies all the requirements for a slow μSR muon source.

The apparatus used for this work is shown below in figure (35). More details of this important work will be described I believe by other speakers, suffice it for me to say that a similar facility is currently operational at ISIS, where the pulsed nature of the source allows a considerable simplification over the PSI design. We await new and exciting results from these new low energy facilities.

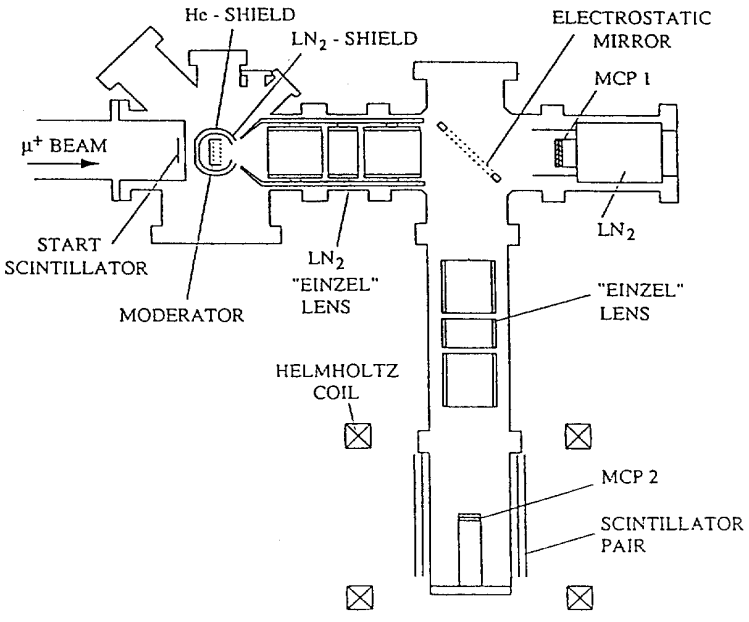

Fig. 35: Lay-out of the PSI Slow Muon Facility. The principal component consists of a UHV system containing a cryostat and electrostatic grids, mirrors and einzel lenses.

The Future: Muon Facilities in the New Millennium

For the sake of argument, we can suppose that the three principal muon sources currently in use, ie PSI, TRIUMF and ISIS, will continue to operate for the next 10 - 15 years. Where will we do muon experiments after that? Fortunately for us, new and more powerful facilities are in the pipeline and here I will describe two of them and what sort of muon facilities and improvements they will provide. One of these, the Japanese Hadron Facility will be in Japan, while the other, The European Spallation source will be located somewhere in Europe, but as yet I know not where, hopefully the South of France or Tuscany perhaps.

The Japanese Hadron Facility

This ambitious accelerator project is shown in figure (36). This project will satisfy the multitude of needs of neutron and muon users fed from a 3 GeV, 200 μA proton beam shown in the figure, which is generated from a 200 MeV Linac and 3 GeV fast cycling synchnotron complex. This beam is further accelerated in a 50 GeV synchnotron to satisfy the needs of high energy physics.

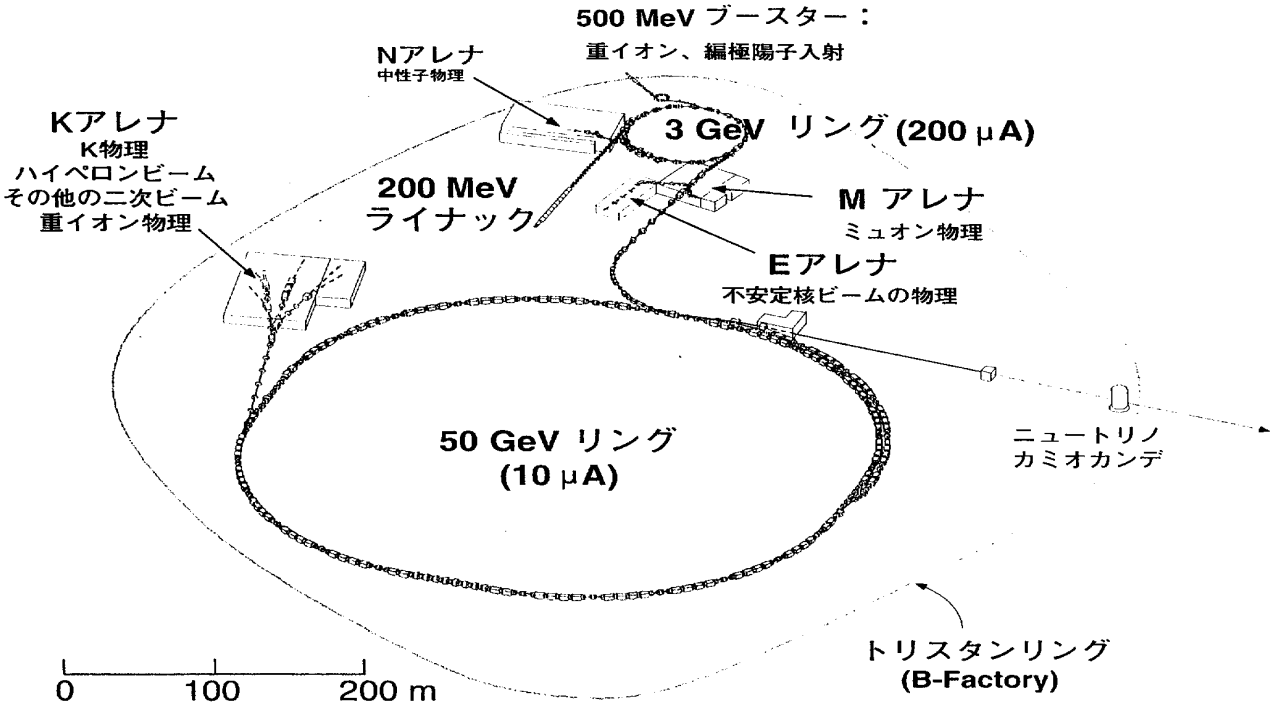

Fig. 36: Layout of the proposed Japanese Hadron Facility.

A comparison between JHF, ESS and ISIS accelerators is given in table below

Facility	Energy (GeV)	Protons/pulse	Repetition rate (Hz)	Current (μA)
ISIS	0.8	$2.5\ 10^{13}$	50	200
JHF	3.0	$5.0\ 10^{13}$	25	200
ESS	1.33	$9.4\ 10^{14}$	50	3770

One can readily see that the principal advantages which JHF has over ISIS given that the proton currents are identical, is the higher energy (3 GeV to 0.8 GeV). Combining this with twice the

protons/pulse at half the repetition rate, means that JHF muon beams will be significantly (x 5-10) higher instantaneous rates than ISIS. The JHF will have similar time structure to ISIS, so that the muon facilities which are proposed can incorporate a number of kicker magnets to multiplex many beams from a single production target. The proposed muon complex, is shown in figure (37) and comprises surface and decay muon channels serving a total of ten experimental areas. This will be a very powerful facility allowing a continuation of muon science at least in Japan.

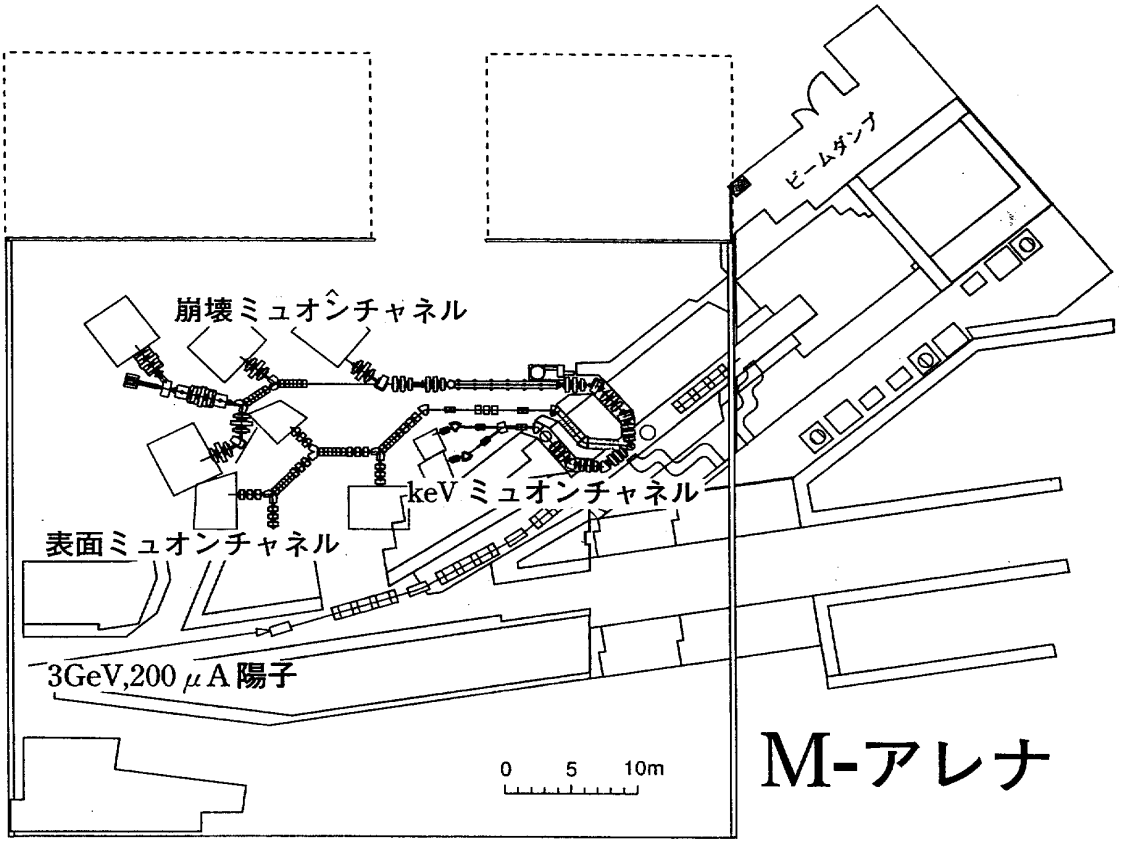

Fig. 37: The proposed Muon Facilities at the JHF.

The European Spallation Source (ESS). [51]

The proposed ESS is the next generation spallation neutron source for Europe and will mark a major advance upon the performance of ISIS. The accelerator consists of a 1.334 GeV Linac feeding continuous proton beams into an accumulator ring where bunching occurs to two proton bunches each 400 ns long, within 1 μsec total length. This 5 MW proton beam is then extracted as in figure (38).

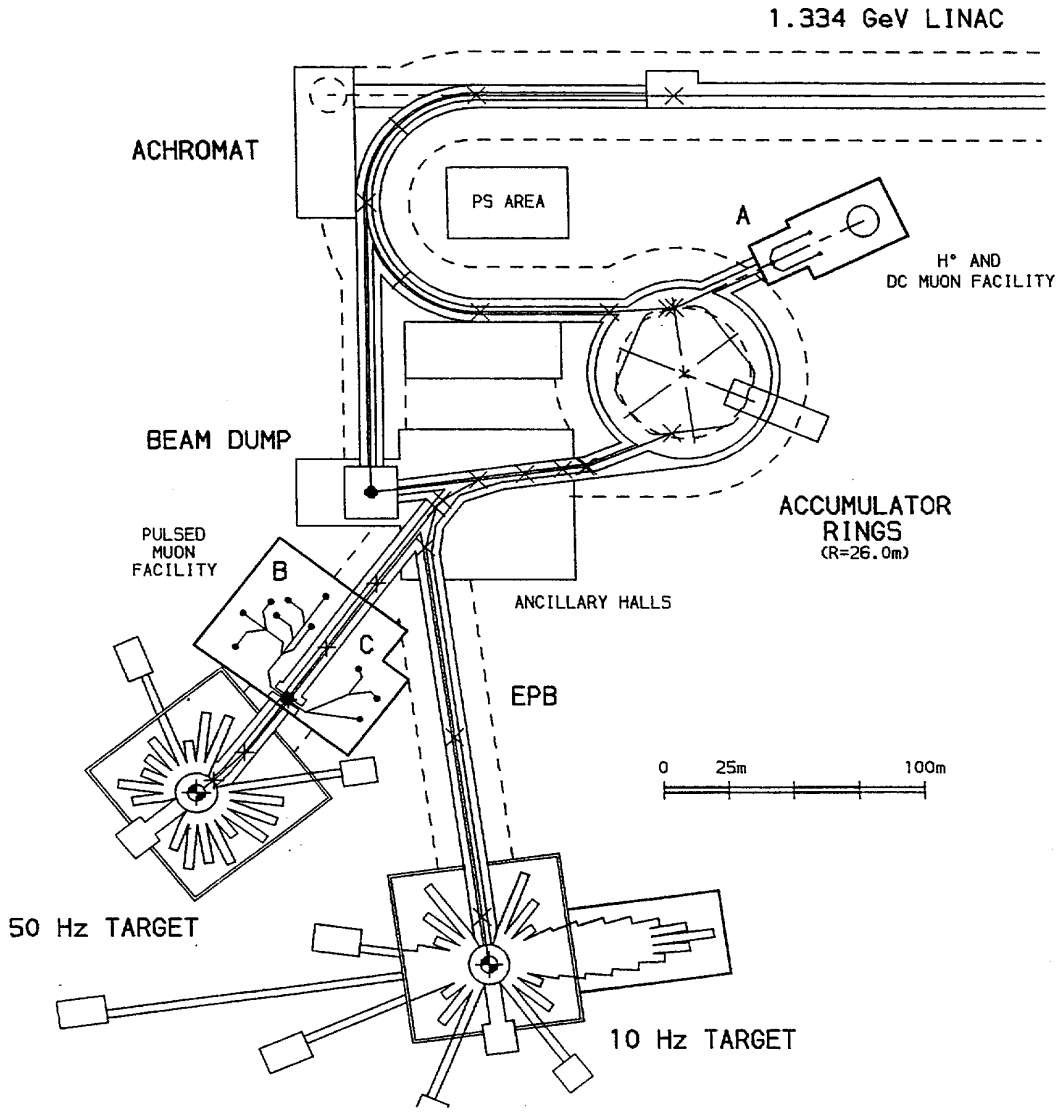

Fig. 38: The European Spallation Source: Layout of Accelerators and Beam Lines.

to a 50 Hz 5MW or 10 Hz 1 MW target station. The parameters for the 50 Hz proton beams are shown in the previous table. The 50 Hz neutron source will be x 30 times brighter than the ISIS source, representing a enormous increase in potential for neutron (and muon) science.

One can see in the above figure, two areas for muon facilities. One of these is located in the pulsed 50 Hz proton beam from which very intense muon beams can be generated using a complex shown in figure (39).

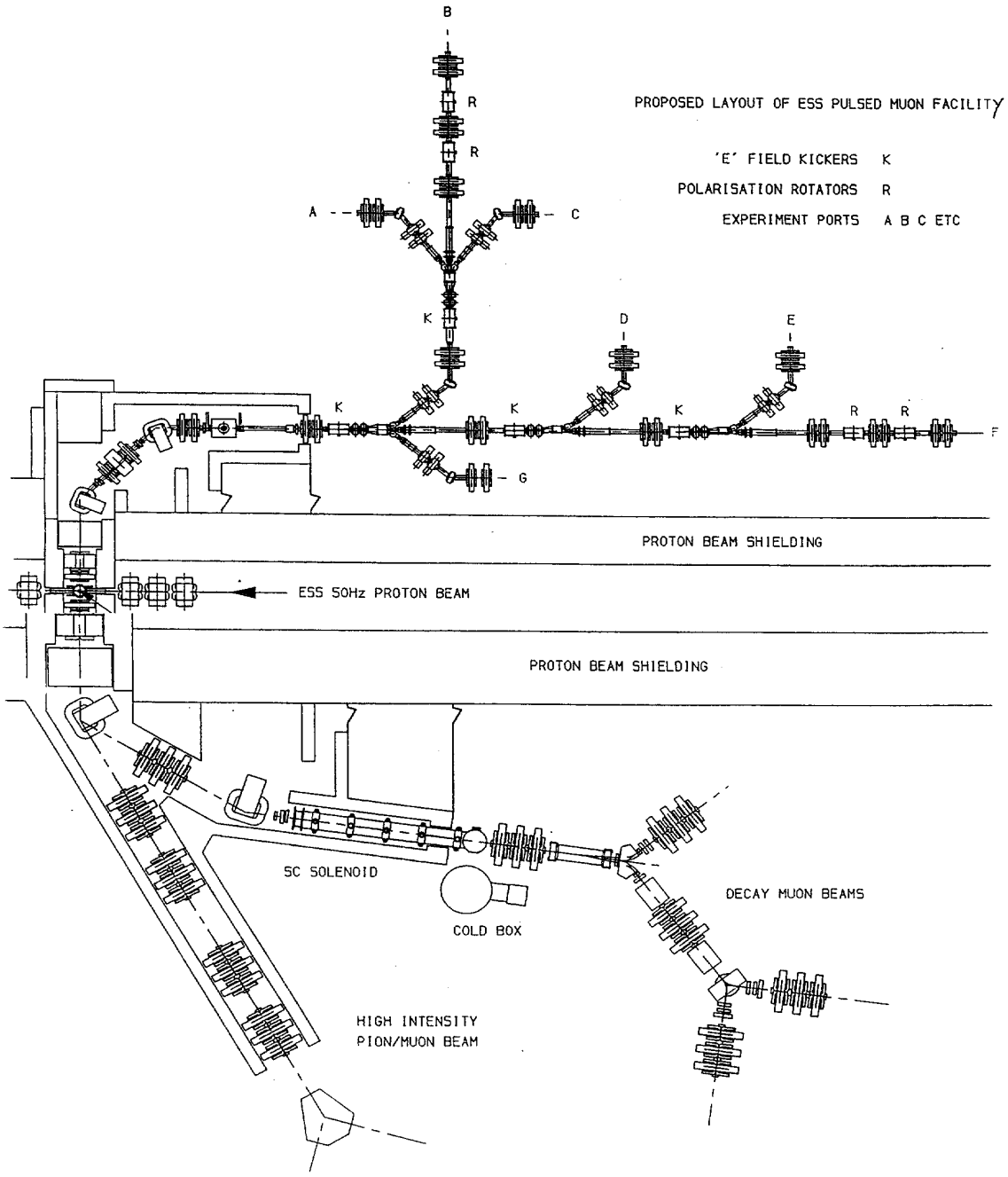

Fig. 39: The Pulsed Pion/Muon and Decay Muon Beam from the ESS.

Because of the increased pulse length of the ESS proton pulse, fast kicker magnets can be used within the pulse itself as well as between pulses to produce six surface muon areas with single muon pulses of variable time width. (Top complex in figure 39). Further decay beams and a high intensity pion/muon channel would be fed from the same target station, to give a total of thirteen areas with simultaneous single muon pulses and a further two areas where muons could be switched on a longer time scale. The improvement in these beams over ISIS is clearly indicated by figure (40), which compares the ESS muon pulse with that from ISIS. Such enormous increases would necessitate development of new detection techniques.

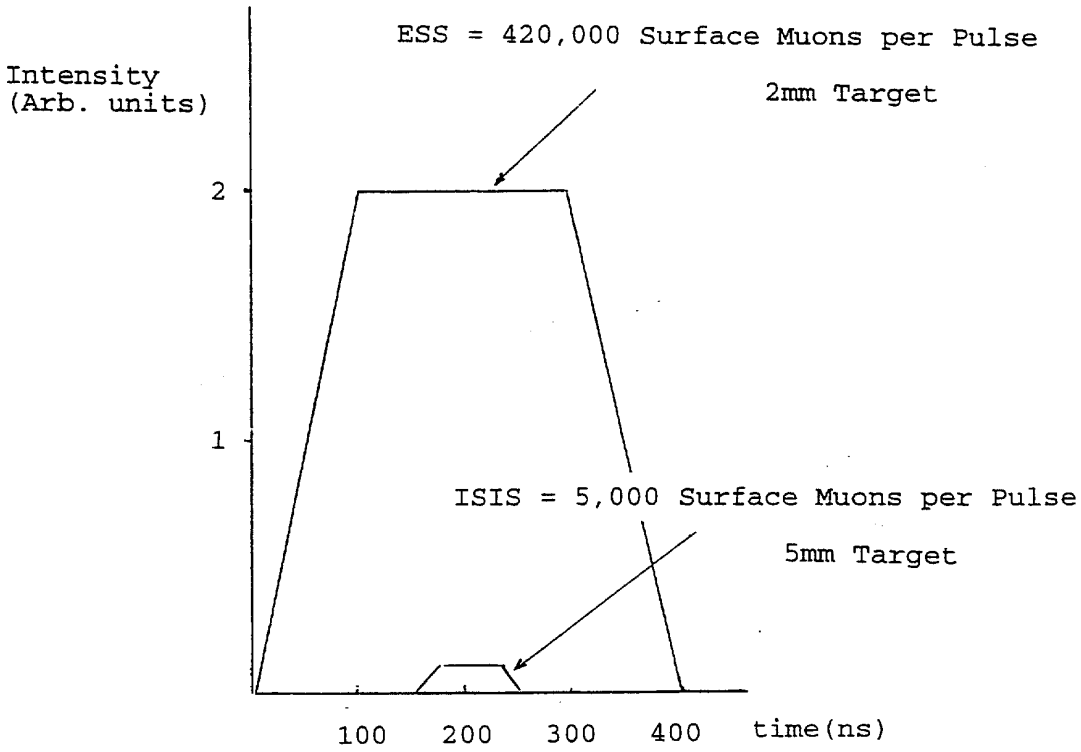

Fig. 40: Comparison between ESS and ISIS Surface Muon Intensities and Time Structure

This pulsed facility would be complemented by a continuous muon facility located in the stripped H^- beam shown in figure (38). Two surface muon channels would be competitive in intensity to PSI beams but would benefit from the smaller emittance of the ESS proton beam, allowing smaller final muon spots at the sample.

Conclusion

Future construction of ESS and JHF will provide muon facilities for our young audience to continue the pioneering work carried out over the last forty years at many laboratories throughout the world. I personally wish them all well in this exciting branch of physics and have to express a little envy on the quality of the facilities which the future will bring.

Acknowledgements

I would like to thank Chris Scott for allowing me to use some of his material for this report. In a small way, I would like to dedicate this report to my colleagues at RAL and in the international muon community who have contributed so much in realizing the worlds most powerful pulsed muon source at ISIS.

References

[1] Kunze, P. Z. Phys. 83 (1933) 1.

[2] Neddermeyer, S. H. and Anderson, C. D. Phys. Rev. 51 (1937) 884.

[3] Yukawa, H. Proc. Phys. Math. Soc. Japan 17 48 (1935).

[4] Conversi, M., Pancini, E. and Piccioni, O. Phys. Rev. 71 209 (1947).

[5] Sakata, S. and Inoue, T. Progr. Theor. Phys. 1 143 (1946).

[6] Lattes, C. M. G., Muirhead, H., Occhialini, G. P. S. and Powell, C. F. Nature 159 694 (1947).

[7] Wu, C. S. and Hughes, V. W. Muon Physics Academic Press, New York (1977).

[8] Scheck, F., Phys. Reports 44 (1978) 187.

[9] Guzhavin, V. M. et al. Soviet Phys. JETP 19 847 (1964).

[10] Alexander, G et al. Phys. Rev. 154 1284 (1967)

[11] Alexander, G. et al. Nuclear PhysicsB5 1 (1969)

[12] Particle Data Group, Phys. Letters 75B1 (1978).

[13] Daum, M., Eaton, G. H., Frosch, R., Hirschmann, H., McCulloch, J., Minehart, R. C. and Steiner, E., Phys. Rev. D. 20 2692 (1979)

[14] Carrigan, R. A., Nuclear Physics B6 662 (1968).

[15] Michel, F. C., Proc. Phys. Soc. (London) A63. 514 and 1371 (1950).

[16] Garwin, Ledermann and Weinrich. Phys. Rev. 105 1415 (1957).

[17] Jones, S. E., Nature 321 127 (1986).

[18] Marshall, G. M. Z. Phys. C. 56 S226 (1991).

[19] Abela, R., Foroughi, F. and Renker, D., Z. Phys. C. 56 S240 (1991).

[20] Nagamine K., Z. Phys. C56 S215 (1991).

[21] Eaton, G. H., Z. Phys. C56 S232 (1991).

[22] Eaton, G. H., Carne, A., Reading, D. H. and Sandels, E. G., Nucl. Inst. and Methods 214 151 (1983).

[23] Piper, A. E., Bowen, T., Kendall, K. R., Nucl. Inst. Meth. 135 (1976) 39.

[24] SIN Users Handbook 39 (1981).

[25] Eaton, G. H., Carne, A., Cox, S. F. J., Davies, J. D., De Renzi, R., Hartmann, O., Kratzer, A., Ristori, C., Scott, C. A., Stirling, G. C. and Sundquist, T., Nucl. Inst. and Meth. A269 (1988) 483.

[26} Borden, A. I., Carne, A., Clarke-Gather, M. A., Eaton, G. H., Jones, H. J., Thomas, G., Hartmann, O. and Sundquist, T., Nucl. Inst. and Meth. A292 (1990) 21.

[27] Eaton, G. H., Clarke-Gayther, M. A., Scott, C. A., Uden, C. N., Williams, W. G., Nucl. Inst. and Meth. A342 (1994) 319.

[28] Eaton, G. H., Scott, C. A. and Williams, W. G., Proc. Int. Workshop on Low Energy Muon Science LEMS '93 Los Alamos LA-12698-C (1993).

[29] RIKEN-RAL Muon Facility Report 1. (1997).

[30] Nagamine, K., Matsuzaki, T., Ishida, K, Watanabe, I., Kadono, R., Eaton, G. H., Jones, H. J., Thomas, G., Williams, W. G., Proc. Int. Workshop on Low Energy Muon Science Los Alamos LA-12698-C Los Alamos (1993).

[31] Daum, M. Nucl. Inst. and Meths. 192 (1982) 137.

[32] Techniques for Nuclear and Particle Physics Experiments. W R Leo. Springer-Verlag 1987.

[33] Coffin, T., Garwin, R.L., Penman, S., Ledermann, L., Sachs, A.M. Phys. Rev. 109 (1958) 973.

[34] Katanka et al. Hyperfine Interactions 12 (1982) 51.

[35] Sugai, T., Kondow, T., Matsushita, A., Nishayama, K., Nagamine, K., Chemical Phys. Letters 188 (1992) 100.

[36] Azuma, T., Nishiyama, K., Nagamine, K., Ito, Y., Tabata, Y., Hyperfine Interactions 32 (1986) 837.

[37] Kreitzmann, S.R., Hyperfine Interactions. 65 (1990) 1055.

[38] Hampele, M., Kratzer, A., Maier, K., Major, J., Münch, K.H. and Th. Pfiz. Proceedings of 6th Int. Conf. On Muon Spin Rotation, Maui Hawaii (1994).

[39] Blazey, K.W., Estle, T.L., Rudaz, S.L., Holzschuh, E., Kündig, W. and Patterson, B.D. Phys. Rev. B34 3 (1986) 1422.

[40] Kreitzmann, S.R., Hitti, B., Lichti, R., Estle, T.L. and Chow, K.H. (to be published).

[41] Carne, A., Cox, S.F.T., Eaton, G.H., DeRenzi, R., Scott, C.A., Stirling, G.C. Hyp. Interations 17-19 (1984) 945.

[42] Cottrell, S.P., Scott, C.A. and Hitti, B. Hyperfine Interactions 106 (1997) 251.

[43] Yamazaki, T., Hayano, R.S., Kuno, Y., Ohtake, S. and Nagae, T. Nucl. Inst. and Methods 196 (1982) 289.

[44] Hampele, M., Herlach, D., Kratzer, A., Majer, G., Major, J., Raich, H.P., Roth, R., Scott, C.A., Seeger, A., Templ, W., Blanz, M., Cox, S.F.J. and Fürdere. Hyperfine Interactions 65 (1990) 1082.

[45] Jones, S.E., Nature 321 (1986) 127.

[45] RIKEN-RAL Muon Facility Report (1995 - 1997) Volume 1 1997.

[47] Maas F.E. et al. Physics Letters A187 (1994) 247.

[48] Schwarz, W. et al. IFEE transactions on Instrumentation and Measurement. 44 (1995) 505.

[49] Harshman, D.R., Warren, J.B., Beveridge, J.L., Kendall, C.R., Kiefl, R.F., Oram, C.J., Mills, A.P., Crane, W.S., Rupaal, A.S. and Turner, J.H. Phys. Rev. Letters 56 (1986) 2850.

[50] Morenzoni, E., Kottmann, F., Maden, D., Matthias, B., Meyberg, M., Protscha, Th., Wutzke, T., Zimmermann, V. Phys. Rev. Letters 72 (1994) 2793.

[51] Gardner, I.S.K., Lengeler, H. and Rees, G.H. ESS Report ESS/P1/1995.